

The public reporting burden for this collection of information is estimated to average 1 hour per response, including the time for reviewing instructions, searching existing data sources, gathering and maintaining the data needed, and completing and reviewing the collection of information. Send comments regarding this burden estimate or any other aspect of this collection of information, including suggestions for reducing this burden, to Washington Headquarters Services, Directorate for Information Operations and Reports, 1215 Jefferson Davis Highway, Suite 1204, Arlington VA, 22202-4302. Respondents should be aware that notwithstanding any other provision of law, no person shall be subject to any penalty for failing to comply with a collection of information if it does not display a currently valid OMB control number.  
PLEASE DO NOT RETURN YOUR FORM TO THE ABOVE ADDRESS.

1. REPORT DATE (DD-MM-YYYY) 29-11-2016	2. REPORT TYPE Final Report	3. DATES COVERED (From - To) 1-Sep-2013 - 31-Aug-2016
---	--------------------------------	--

4. TITLE AND SUBTITLE Final Report: Fabrication of Complex-Shaped Ceramic Components by Room-Temperature Injection Molding of Ceramic Suspension Gels	5a. CONTRACT NUMBER W911NF-13-1-0425
	5b. GRANT NUMBER
	5c. PROGRAM ELEMENT NUMBER 611102

6. AUTHORS Prof. Rodney Trice, Prof. Jeffrey Youngblood	5d. PROJECT NUMBER
	5e. TASK NUMBER
	5f. WORK UNIT NUMBER

7. PERFORMING ORGANIZATION NAMES AND ADDRESSES Purdue University 155 South Grant Street  West Lafayette, IN 47907 -2114	8. PERFORMING ORGANIZATION REPORT NUMBER
---	--

9. SPONSORING/MONITORING AGENCY NAME(S) AND ADDRESS (ES) U.S. Army Research Office P.O. Box 12211 Research Triangle Park, NC 27709-2211	10. SPONSOR/MONITOR'S ACRONYM(S) ARO
	11. SPONSOR/MONITOR'S REPORT NUMBER(S) 63029-MS.5

12. DISTRIBUTION AVAILABILITY STATEMENT Approved for Public Release; Distribution Unlimited
--

13. SUPPLEMENTARY NOTES The views, opinions and/or findings contained in this report are those of the author(s) and should not be construed as an official Department of the Army position, policy or decision, unless so designated by other documentation.
---

14. ABSTRACT Novel forming of ceramics into complex shapes of silicon nitride (Si3N4) and boron carbide (B4C) has been investigated. Common to our approach was to use a polymer in the ceramic-loaded suspensions. The polymer employed was flowable at room-temperature, water soluble, imparted green strength to the formed body, and in some cases, acted as a dispersing agent. Lisa Rueschhoff developed suspensions of silicon nitride powders. She was able to show that that water reducing admixtures used in concrete are effective for dispersing Si3N4 in water. These suspensions have been injection molded. Andres Diaz Carr has investigated preparation of aqueous
--

15. SUBJECT TERMS boron carbide, silicon nitride, ceramic processing, sintering
--

16. SECURITY CLASSIFICATION OF:	17. LIMITATION OF ABSTRACT	15. NUMBER OF PAGES	19a. NAME OF RESPONSIBLE PERSON Rodney Trice
a. REPORT UU	b. ABSTRACT UU	c. THIS PAGE UU	19b. TELEPHONE NUMBER 765-494-6405

## Report Title

Final Report: Fabrication of Complex-Shaped Ceramic Components by Room-Temperature Injection Molding of Ceramic Suspension Gels

### ABSTRACT

Novel forming of ceramics into complex shapes of silicon nitride (Si<sub>3</sub>N<sub>4</sub>) and boron carbide (B<sub>4</sub>C) has been investigated. Common to our approach was to use a polymer in the ceramic-loaded suspensions. The polymer employed was flowable at room-temperature, water soluble, imparted green strength to the formed body, and in some cases, acted as a dispersing agent. Lisa Rueschhoff developed suspensions of silicon nitride powders. She was able to show that that water reducing admixtures used in concrete are effective for dispersing Si<sub>3</sub>N<sub>4</sub> in water. These suspensions have been injection molded. Andres Diaz Cano has investigated preparation of aqueous suspensions of boron carbide powders, achieving up to 56 vol.% B<sub>4</sub>C powder loadings. He has also studied the best sintering aids to density B<sub>4</sub>C without external pressure at low temperatures (2000oC). We were fortunate enough to win both a URAP and HRAP awards for the summer of 2015. In this work, we developed suspensions of alumina (Al<sub>2</sub>O<sub>3</sub>) and boron carbide, and used a syringe-style additive manufacturing approach to print complex shapes. William Costakis was the undergraduate awardee, while Alycia McEachen was the high student student awardee. As a team they were very successful using a 3D printing process to make B<sub>4</sub>C parts.

---

**Enter List of papers submitted or published that acknowledge ARO support from the start of the project to the date of this printing. List the papers, including journal references, in the following categories:**

**(a) Papers published in peer-reviewed journals (N/A for none)**

Received          Paper

**TOTAL:**

**Number of Papers published in peer-reviewed journals:**

---

**(b) Papers published in non-peer-reviewed journals (N/A for none)**

Received          Paper

**TOTAL:**

**Number of Papers published in non peer-reviewed journals:**

---

**(c) Presentations**

1. L. Rueschhoff\*, J. Youngblood, R. Trice (2016) "Room-Temperature and Low-Pressure Injection Molding of Silicon Nitride Aqueous Suspensions" Oral Presentation to be presented at MS&T, Salt Lake City, Utah.
2. L. Rueschhoff\*, J. Youngblood, R. Trice (2016) "Ceramic Near-Net Shaped Processing via Highly-Loaded Aqueous Suspensions" Invited Presentation at U.S. Army Research Laboratory (ARL), Aberdeen Proving Ground, Maryland.
3. L. Rueschhoff\*, J. Youngblood, R. Trice (2016) "Room-Temperature Injection Molding of Silicon Nitride Aqueous Suspensions" Poster Presentation at the 2016 Gordon Research Seminar and Conference on Solid State Studies in Ceramics, South Hadley, Massachusetts.
4. A. Diaz-Cano\*, J. Youngblood, R. Trice (2016) "Room-temperature injection molding of boron carbide" - Poster Presentation at the 2016 Gordon Research Seminar and Conference on Solid State Studies in Ceramics, South Hadley, Massachusetts.
5. L. Rueschhoff\*, J. Youngblood, R. Trice (2016) "Room-Temperature and Low-Pressure Injection Molding of Silicon Nitride Aqueous Suspensions" Invited Presentation at NASA Glenn Research Center, Cleveland, Ohio.
6. A. Diaz-Cano\*, J. Youngblood, R. Trice (2016) "Optimization of water based boron carbide suspension gels" Oral Presentation at the ACerS International Conference & Exposition on Advanced Ceramics & Composites (ICACC), Daytona Beach, FL.
7. L. Rueschhoff\*, J. Youngblood, R. Trice (2016) "Manufacturing Complex-Shaped Silicon Nitride Components with Aligned Microstructural Features through Room-Temperature Injection Molding and 3D Printing of Ceramic Suspension Gels (CeraSGels)" Oral Presentation at ICACC, Daytona Beach, FL.
8. L. Rueschhoff\*, J. Youngblood, R. Trice (2016) "The Use of Concrete Admixtures to Disperse Highly Loaded Silicon Nitride Ceramic Suspension Gels (CeraSGels) for Room-Temperature Processing" Oral Presentation at ICACC, Daytona Beach, FL.
9. W. Costakis\*, A. Diaz Cano, L. Rueschhoff, A. McEachen, R. Trice, J. Youngblood (2016) "Optimization of Boron Carbide Ceramic Suspension Gels (CeraSGels) for Room Temperature Robocasting" Oral Presentation at ICACC, Daytona Beach, FL.
10. V. Wiesner\*, L. Rueschhoff, M. Acosta, J. Youngblood, R. Trice (2016) "Manufacture of complex-shaped ceramic components with highly oriented reinforcing phase by horizontal dip-spin casting." Oral Presentation at ICACC, Daytona Beach, FL.
11. L. Rueschhoff\*, J. Youngblood, R. Trice (2015) "Fabricating Complex-Shaped Ceramic Components through Novel Room-Temperature Injection Molding and 3D Printing of Ceramic Powder Suspension Gels (CeraSGels)" Oral Presentation at MS&T, Columbus, OH.
12. L. Rueschhoff\*, W. Costakis, M. Michie, A. Diaz-Cano, J. Youngblood, R. Trice (2015) "Manufacturing Complex-Shaped Ceramic Components through Room-Temperature Robocasting of Ceramic Suspension Gels (CeraSGels)" Oral Presentation at MS&T, Columbus, OH.
13. A. Diaz-Cano\*, J. Youngblood, R. Trice (2015) "Room Temperature Injection Molding of Water-Based Boron Carbide Suspensions" Oral Presentation at MS&T, Columbus, OH.
14. L. Rueschhoff\*, J. Youngblood, R. Trice (2015) "Fabrication of Complex-Shaped Ceramic Components through Novel Room-Temperature Injection Molding and 3D Printing of Ceramic Powder Suspension Gels (CeraSGels)" Oral Presentation and Poster at TMS, Orlando, FL.
15. A. Diaz-Cano\*, J. Youngblood, R. Trice (2015) "Optimization of water based boron carbide suspensions for room-temperature injection molding to produce complex-shaped armor components" Oral Presentation at ICACC, Daytona Beach, FL.
16. L. Rueschhoff\*, J. Youngblood, R. Trice (2015) "Manufacturing Complex-Shaped Ceramic Components with Aligned Microstructural Features through Room-Temperature Injection Molding and 3D Printing of Ceramic Suspension Gels (CeraSGels)" Oral Presentation at ICACC, Daytona Beach, FL.
17. L. Rueschhoff\*, A. Diaz-Cano, M. Michie, V. Wiesner, J. Youngblood, R. Trice (2015) "3D Printing of Ceramic Suspension Gels (CeraSGels) to Produce Ceramic Components with Near-Net Shape Geometries" Oral Presentation at ICACC, Daytona Beach, FL.
18. L. Rueschhoff\*, J. Youngblood, R. Trice (2014) "Alignment of Microstructural Features in Ceramics through Injection Molding of Ceramic Suspension Gels (CeraSGels) at Room Temperature" Poster presentation at MS&T, Pittsburgh, PA.

**Number of Presentations:** 18.00

---

**Non Peer-Reviewed Conference Proceeding publications (other than abstracts):**

Received

Paper

**TOTAL:**

Number of Non Peer-Reviewed Conference Proceeding publications (other than abstracts):

---

**Peer-Reviewed Conference Proceeding publications (other than abstracts):**

Received      Paper

**TOTAL:**

Number of Peer-Reviewed Conference Proceeding publications (other than abstracts):

---

**(d) Manuscripts**

Received      Paper

**TOTAL:**

Number of Manuscripts:

---

**Books**

Received      Book

**TOTAL:**

Received

Book Chapter

**TOTAL:**

**Patents Submitted**

Injection Molding of Aqueous Suspensions of High-Temperature Ceramics (USPTO# 62/184,292)

---

**Patents Awarded**

---

**Awards**

Honors and Awards:

Lisa Rueschhoff

---

- o ACerS Graduate Excellence in Materials Science Award Finalist, 2016
  - o Purdue University College of Engineering Magoon Award for Excellence in Teaching, 2016
  - o ASM Indianapolis Chapter Purdue Student Night Best Poster Award, 2016
  - o Council Chair for the ACerS President's Council of Student Advisors, 2015-2016
  - o NSF Graduate Research Fellowship Program (GRFP), 2014-2017
- 

**Graduate Students**

<u>NAME</u>	<u>PERCENT SUPPORTED</u>
<b>FTE Equivalent:</b>	
<b>Total Number:</b>	

---

**Names of Post Doctorates**

<u>NAME</u>	<u>PERCENT SUPPORTED</u>
<b>FTE Equivalent:</b>	
<b>Total Number:</b>	

---

**Names of Faculty Supported**

<u>NAME</u>	<u>PERCENT SUPPORTED</u>
<b>FTE Equivalent:</b>	
<b>Total Number:</b>	

---

**Names of Under Graduate students supported**

<u>NAME</u>	<u>PERCENT SUPPORTED</u>
<b>FTE Equivalent:</b>	
<b>Total Number:</b>	

**Student Metrics**

This section only applies to graduating undergraduates supported by this agreement in this reporting period

The number of undergraduates funded by this agreement who graduated during this period: ..... 2.00

The number of undergraduates funded by this agreement who graduated during this period with a degree in science, mathematics, engineering, or technology fields:..... 2.00

The number of undergraduates funded by your agreement who graduated during this period and will continue to pursue a graduate or Ph.D. degree in science, mathematics, engineering, or technology fields:..... 1.00

Number of graduating undergraduates who achieved a 3.5 GPA to 4.0 (4.0 max scale):..... 1.00

Number of graduating undergraduates funded by a DoD funded Center of Excellence grant for Education, Research and Engineering:..... 2.00

The number of undergraduates funded by your agreement who graduated during this period and intend to work for the Department of Defense ..... 0.00

The number of undergraduates funded by your agreement who graduated during this period and will receive scholarships or fellowships for further studies in science, mathematics, engineering or technology fields:..... 0.00

---

**Names of Personnel receiving masters degrees**

<u>NAME</u>
<b>Total Number:</b>

---

**Names of personnel receiving PHDs**

<u>NAME</u>
<b>Total Number:</b>

---

**Names of other research staff**

<u>NAME</u>	<u>PERCENT SUPPORTED</u>
<b>FTE Equivalent:</b>	
<b>Total Number:</b>	

---

**Sub Contractors (DD882)**

**Inventions (DD882)**

**Scientific Progress**

see attachment

## Technology Transfer

Masten Space Systems an aerospace manufacturer startup company currently located in Mojave, California is interested in using the developed room-temperature injection molding process to make cost effective ceramic turbine blade. A three dimensional CAD drawing of the supplied polymer mold is shown in Figure 15a. Based on previous success with alumina (Valerie), zirconium diboride (Valerie), boron carbide (Andres), and silicon nitride (Lisa) it was proposed that room-temperature injection molding of aqueous ceramic suspensions can be used to develop complex shaped (turbine) high temperature ceramic structures. Alumina was selected as a test material to develop the proof of concept due to the ease of use, low cost and optimized rheological properties. Due to the complex nature of the selected mold, the dried suspensions would need a higher green body strength when compared to previous studies. It was determined that a 51 vol.% Al<sub>2</sub>O<sub>3</sub> suspension with 5 vol.% PVP produced the highest final quality specimens. An image of the injection process is shown in Figure 1b. High density alumina turbine blades were successful injection molded. An image of the final product is shown in Figure. 16. In order to reduce drying induce cracking and promote successful removal of the green sample, filter paper was applied to the surface of the mold. Future, work will consist of developing a mold releasing agent that allows for the deconstruction of the mold during the drying process. This is important so that the piece can shrink freely during the drying process.

See attachment for figures!

## Section A

**To:** Dr. David Stepp & Dr. Michael Bakas  
**Subject:** Final Report

**Grant Title:** Fabrication of Complex-Shaped Ceramic Components by Room-Temperature Injection Molding of Ceramic Suspension Gels  
**Grant #:** ARO# W911NF-13-1-0425  
**Reporting Period:** Sept 1, 2013 – August 31, 2016

**PIs:** Prof. Rodney Trice and Prof. Jeffrey Youngblood  
**Performing Organization:** Purdue University, 701 West Stadium Avenue, West Lafayette, IN 47907

### Abstract

Novel forming of ceramics into complex shapes of silicon nitride ( $\text{Si}_3\text{N}_4$ ) and boron carbide ( $\text{B}_4\text{C}$ ) has been investigated. Common to our approach was to use a polymer in the ceramic-loaded suspensions. The polymer employed was flowable at room-temperature, water soluble, imparted green strength to the formed body, and in some cases, acted as a dispersing agent. Lisa Rueschhoff developed suspensions of silicon nitride powders. She was able to show that that water reducing admixtures used in concrete are effective for dispersing  $\text{Si}_3\text{N}_4$  in water. These suspensions have been injection molded. Andres Diaz Cano has investigated preparation of aqueous suspensions of boron carbide powders, achieving up to 56 vol.%  $\text{B}_4\text{C}$  powder loadings. He has also studied the best sintering aids to density  $\text{B}_4\text{C}$  *without* external pressure at low temperatures (2000°C). We were fortunate enough to win both a URAP and HRAP awards for the summer of 2015. In this work, we developed suspensions of alumina ( $\text{Al}_2\text{O}_3$ ) and boron carbide, and used a syringe-style additive manufacturing approach to print complex shapes. William Costakis was the undergraduate awardee, while Alycia McEachen was the high student student awardee. As a team they were very successful using a 3D printing process to make  $\text{B}_4\text{C}$  parts.

## Section B

### (1) Submissions and Publications

#### Presentations:

1. L. Rueschhoff\*, J. Youngblood, R. Trice (2016) "Room-Temperature and Low-Pressure Injection Molding of Silicon Nitride Aqueous Suspensions" Oral Presentation to be presented at MS&T, Salt Lake City, Utah.
2. L. Rueschhoff\*, J. Youngblood, R. Trice (2016) "Ceramic Near-Net Shaped Processing via Highly-Loaded Aqueous Suspensions" Invited Presentation at U.S. Army Research Laboratory (ARL), Aberdeen Proving Ground, Maryland.
3. L. Rueschhoff\*, J. Youngblood, R. Trice (2016) "Room-Temperature Injection Molding of Silicon Nitride Aqueous Suspensions" Poster Presentation at the 2016 Gordon Research Seminar and Conference on Solid State Studies in Ceramics, South Hadley, Massachusetts.
4. A. Diaz-Cano\*, J. Youngblood, R. Trice (2016) "Room-temperature injection molding of boron carbide" - Poster Presentation at the 2016 Gordon Research Seminar and Conference on Solid State Studies in Ceramics, South Hadley, Massachusetts.
5. L. Rueschhoff\*, J. Youngblood, R. Trice (2016) "Room-Temperature and Low-Pressure Injection Molding of Silicon Nitride Aqueous Suspensions" Invited Presentation at NASA Glenn Research Center, Cleveland, Ohio.
6. A. Diaz-Cano\*, J. Youngblood, R. Trice (2016) "Optimization of water based boron carbide suspension gels" Oral Presentation at the ACerS International Conference & Exposition on Advanced Ceramics & Composites (ICACC), Daytona Beach, FL.
7. L. Rueschhoff\*, J. Youngblood, R. Trice (2016) "Manufacturing Complex-Shaped Silicon Nitride Components with Aligned Microstructural Features through Room-Temperature Injection Molding and 3D Printing of Ceramic Suspension Gels (CeraSGels)" Oral Presentation at ICACC, Daytona Beach, FL.
8. L. Rueschhoff\*, J. Youngblood, R. Trice (2016) "The Use of Concrete Admixtures to Disperse Highly Loaded Silicon Nitride Ceramic Suspension Gels (CeraSGels) for Room-Temperature Processing" Oral Presentation at ICACC, Daytona Beach, FL.
9. W. Costakis\*, A. Diaz Cano, L. Rueschhoff, A. McEachen, R. Trice, J. Youngblood (2016) "Optimization of Boron Carbide Ceramic Suspension Gels (CeraSGels) for Room Temperature Robocasting" Oral Presentation at ICACC, Daytona Beach, FL.
10. V. Wiesner\*, L. Rueschhoff, M. Acosta, J. Youngblood, R. Trice (2016) "Manufacture of complex-shaped ceramic components with highly oriented reinforcing phase by horizontal dip-spin casting." Oral Presentation at ICACC, Daytona Beach, FL.
11. L. Rueschhoff\*, J. Youngblood, R. Trice (2015) "Fabricating Complex-Shaped Ceramic Components through Novel Room-Temperature Injection Molding and 3D Printing of Ceramic Powder Suspension Gels (CeraSGels)" Oral Presentation at MS&T, Columbus, OH.
12. L. Rueschhoff\*, W. Costakis, M. Michie, A. Diaz-Cano, J. Youngblood, R. Trice (2015) "Manufacturing Complex-Shaped Ceramic Components through Room-Temperature Robocasting of Ceramic Suspension Gels (CeraSGels)" Oral Presentation at MS&T, Columbus, OH.
13. A. Diaz-Cano\*, J. Youngblood, R. Trice (2015) "Room Temperature Injection Molding of Water-Based Boron Carbide Suspensions" Oral Presentation at MS&T, Columbus, OH.

14. L. Rueschhoff\*, J. Youngblood, R. Trice (2015) "Fabrication of Complex-Shaped Ceramic Components through Novel Room-Temperature Injection Molding and 3D Printing of Ceramic Powder Suspension Gels (CeraSGels)" Oral Presentation and Poster at TMS, Orlando, FL.
15. A. Diaz-Cano\*, J. Youngblood, R. Trice (2015) "Optimization of water based boron carbide suspensions for room-temperature injection molding to produce complex-shaped armor components" Oral Presentation at ICACC, Daytona Beach, FL.
16. L. Rueschhoff\*, J. Youngblood, R. Trice (2015) "Manufacturing Complex-Shaped Ceramic Components with Aligned Microstructural Features through Room-Temperature Injection Molding and 3D Printing of Ceramic Suspension Gels (CeraSGels)" Oral Presentation at ICACC, Daytona Beach, FL.
17. L. Rueschhoff\*, A. Diaz-Cano, M. Michie, V. Wiesner, J. Youngblood, R. Trice (2015) "3D Printing of Ceramic Suspension Gels (CeraSGels) to Produce Ceramic Components with Near-Net Shape Geometries" Oral Presentation at ICACC, Daytona Beach, FL.
18. L. Rueschhoff\*, J. Youngblood, R. Trice (2014) "Alignment of Microstructural Features in Ceramics through Injection Molding of Ceramic Suspension Gels (CeraSGels) at Room Temperature" Poster presentation at MS&T, Pittsburgh, PA.

*\*Indicates presenting author*

### **Manuscripts:**

1. V. Wiesner, L. Rueschhoff, A. Diaz-Cano, R. Trice, J. Youngblood, "Producing Dense Zirconium Diboride Components by Room-Temperature Injection Molding of Aqueous Ceramic Suspensions" *Ceramics International*, **42** [2] 2750-2760 (2016).
2. L. Rueschhoff, W. Costakis, M. Michie, J. Youngblood, R. Trice, "Additive Manufacturing of Dense Ceramic Parts via Direct Ink Writing of Aqueous Alumina Suspensions" *To be Featured on the Journal Back Cover International Journal of Applied Ceramic Technology*, (2016) In Press (DOI: 10.1111/ijac.12557).
3. W. Costakis, L. Rueschhoff, A. Diaz-Cano, R. Trice, J. Youngblood, "Additive Manufacturing of Boron Carbide via Continuous Filament Direct Ink Writing of Aqueous Ceramic Suspensions" *Journal of the European Ceramic Society*, **36** [14] 3249-3256 (2016).
4. L. Rueschhoff, J., Youngblood, R. Trice, "Stabilizing Highly-Loaded Silicon Nitride Aqueous Suspensions using Comb Polymer Concrete Superplasticizers" *Journal of the American Ceramic Society*, (2016) In Press (DOI:10.1111/jace.14432).
5. L. Rueschhoff, J. Youngblood, R. Trice, "Room-Temperature Injection Molding of Aqueous Silicon Nitride Suspensions" *In preparation* (2016).
6. A. Diaz-Cano, J. Youngblood, R. Trice, "Preparation Highly-Loaded Boron Carbide Suspensions" *In preparation* (2016).
7. A. Diaz-Cano, J. Youngblood, R. Trice, "Effect of Sintering Aid Type and Concentration on Low Temperature Pressureless Sintering of Boron Carbide." *In preparation* (2016).
8. A. Diaz-Cano, J. Youngblood, R. Trice, "Injection Molding of Boron Carbide Using Aqueous Suspensions." *In preparation* (2016).

**Books:** None

**Honors and Awards:**

*Lisa Rueschhoff*

- ACerS Graduate Excellence in Materials Science Award Finalist, 2016
- Purdue University College of Engineering Magoon Award for Excellence in Teaching, 2016
- ASM Indianapolis Chapter Purdue Student Night Best Poster Award, 2016
- Council Chair for the ACerS President's Council of Student Advisors, 2015-2016
- NSF Graduate Research Fellowship Program (GRFP), 2014-2017

**Title of Patents Disclosed:** Injection Molding of Aqueous Suspensions of High-Temperature Ceramics (USPTO# 62/184,292)

- IP optioned by Masten Space Systems
- Transitioning technology to turbine blade manufacturing with Masten Space Systems

**Patents Awarded:** None

**(2) Student Metrics**

**Graduate Students:** Andres Diaz Cano, Lisa Rueschhoff, Ivan Marino Zuluaga Buritica (visiting student from Universidad Nacional de Colombia in Spring & Summer 2015)

**Undergraduate Students:** William Costakis (URAP 2015, Graduate student beginning in Fall 2015), Benjamin Tims (2015), Eric Coons (2015),

**High School Students:** Alyica McEachen (HRAP)

**(3) Technology Transfer:** None

**(4) Scientific Progress and Accomplishments**

Overview of Project: An investigation of the fundamental processing science to enable injection molding of ceramics via ceramic-suspension gels (CeraSGel) was investigated. A CeraSGel is made by suspending ceramic powders in a gel that is created by dissolving a polymer in water. Rather than control the viscosity (and therefore the flow properties) of the ceramic/polymer mixture through heating and cooling processes as is done in current injection molding operations, the key to the CeraSGel processing approach is to design the rheology of the ceramic/polymer mixture so that forming at room temperature is achievable. Compared to conventional injection molding formulations, very little polymer is required in CeraSGels to achieve the requisite rheology required for forming. For example, in injection molding trials at Purdue University using alumina CeraSGels, only ~2-4 vol% polymer is added compared to the 35 vol% used in conventional injection molding formulations. Because less polymer is required in CeraSGels, binder burnout is faster with fewer residual strength-limiting defects. Also, because CeraSGels use water rather than harsh chemical solvents they are environmentally safe. Application of this

process in its full maturity would influence armor performance, allowing fabrication of integral armor systems and highly curved surfaces with intentionally located microstructural features.

In the work performed here, we took a comprehensive look at all aspects of the CeraSGel process for two new ceramic powder formulations, with the goal of creating dense, defect-free, complex-shaped parts via injection molding. The two material systems, based on  $\text{Si}_3\text{N}_4$  and  $\text{B}_4\text{C}$  powders, were chosen because they represent tough and hard ceramic systems, respectively, each of which can be pressurelessly sintered. In addition, silicon nitride possesses high aspect ratio grains. Our goal was to use the shear stresses during injection molding to influence the grains alignment in the final sintered structure. Boron carbide was of interest because of its use in armor and the relative lack of data related to forming it via injection molding.

Overall, our goal was to be able to process ceramics in a manner similar to polymers, with all of the inherent flexibility in design and lower costs. What follows is a description of the work performed on ARO# W911NF-13-1-0425 from September 1, 2013 through August 31, 2016. Two PhD students worked on this grant, Lisa Rueschhoff and Andres Diaz Cano. Lisa subsequently was awarded a prestigious NSF Graduate Student Fellowship to leverage our efforts. Furthermore, we generously received both URAP and HRAP grants from ARO for this work to support two students in the summer of 2015. William Costakis (URAP) and Alycia McEachen (HRAP) explored 3D printing of  $\text{B}_4\text{C}$  with great success. Both Lisa and Andres will graduate in May, 2017, with more publications expected as indicated in the list above.

## **I. Near-Net Shaping of Silicon Nitride via Highly-Loaded Aqueous Suspensions (Graduate Student: Lisa Rueschhoff)**

### PROJECT GOALS

Silicon nitride ( $\text{Si}_3\text{N}_4$ ) based ceramics have been the focus of research efforts that accelerated in the 1960s due to a search for new materials with good high-temperature mechanical properties and thermal shock resistance.  $\text{Si}_3\text{N}_4$  is promising for gas turbine engine parts, as well as other numerous structural applications due to high flexural strength, fracture resistance, hardness, superior wear resistance, and substantial creep resistance up to 1350 °C. These beneficial properties arise from dense microstructures containing interlocking  $\beta$ - $\text{Si}_3\text{N}_4$  acicular grains that deflect and bridge propagating cracks. Dense  $\text{Si}_3\text{N}_4$  parts have traditionally been made using tape casting and hot pressing, methods that cannot form complex shapes and require multiple costly steps. More complex shaped parts have been made via processes such as gel-casting and injection molding. Gel-casting of  $\text{Si}_3\text{N}_4$  has been accomplished via a cross-linking reaction in slurries with solids loading upwards of 45 vol.%, with dried parts containing approximately 6 wt.% polymer. However, these parts are machined into complex shapes after forming while in their green state. Thus, there is a need for continued development of processing methods to form dense complex-shaped parts of  $\text{Si}_3\text{N}_4$ . This work aims to utilize processing methods capable of producing near-net complex-shaped parts, such as injection molding and direct ink writing manufacturing, along with

highly-loaded aqueous  $\text{Si}_3\text{N}_4$  suspensions. This project aims to use the flow stresses generated during injection molding to locally align  $\beta\text{-Si}_3\text{N}_4$  *seeds*, which in turn will influence the formation of  $\beta\text{-Si}_3\text{N}_4$  *grains* during sintering. The acicular and elongated  $\beta\text{-Si}_3\text{N}_4$  seeds affect the alignment of the new  $\beta\text{-Si}_3\text{N}_4$  grains formed during sintering and contribute to the high toughness of silicon nitride through the deflection and bridging of propagating cracks. Through careful design of the injection mold, with the help of advanced modeling software, we have shown that it is possible to use shear stresses that arise during molding to intentionally orient the final grain structures formed in  $\beta\text{-Si}_3\text{N}_4$ .

#### OVERVIEW OF WORK TO DATE

- $\alpha\text{-Si}_3\text{N}_4$  suspensions have been designed via a novel formulation containing commercially available water reducing admixtures (WRAs) commonly used in the concrete industry. We have achieved  $\text{Si}_3\text{N}_4$  volume loadings up to 47%.
- We have characterized the four best performing WRAs using Fourier transform infrared spectroscopy (FTIR) to understand their chemical structure and effectiveness as a dispersant for silicon nitride. Understanding the structure of WRAs is important to explain the differences in performance as a ceramic powder dispersant.
- These  $\text{Si}_3\text{N}_4$  suspensions have been used to injection mold and cast parts that have been sintered to high densities in our lab. Microstructural and x-ray analysis confirms these sintered parts have fully transformed into  $\beta\text{-Si}_3\text{N}_4$ , a phase necessary for the robust mechanical properties desired.
- Preliminary work on additive manufacturing using these  $\text{Si}_3\text{N}_4$  suspensions has been carried out at NASA Glenn Research Center using their nScrypt syringe style 3D printer. Results show the feasibility of these suspensions as inks for direct ink writing 3D printing process, but further rheology optimization is needed for build-up of layers.
- Past work was done to both produce and optimize the formation of  $\beta\text{-Si}_3\text{N}_4$  seeds in our lab, as well as quantification of alignment during injection molding through advanced simulation software (Moldex3D) that calculates shear stresses. Current work focuses on utilizing the shear stresses during mold filling and direct ink writing to align  $\beta\text{-Si}_3\text{N}_4$  seeds and therefore  $\beta\text{-Si}_3\text{N}_4$  grains after sintering.

#### STABILIZING AQUEOUS SILICON NITRIDE SUSPENSIONS USING COMB POLYMER CONCRETE SUPERPLASTICIZERS

Commercially available WRAs are used in the concrete industry to disperse cementitious particles in order to reduce the water to cement (w/c) ratio allowing for higher strength concrete or increased workability (i.e. lower viscosity). While the precise chemical make-up of each WRA is proprietary, the base structure for most WRAs is a synthetic comb-polymer. They are typically composed of an anionic main chain (often polyacrylic acid, PAA) with neutral side chains (polyethylene oxide, PEO). The charged main chain attaches to charged particles, while the neutral side chains act to physically repel other particles (steric hindrance) in order to stabilize the suspension, as shown in Figure 1. These WRAs have extensively been studied as cement dispersants, but no work has been

done applying them as ceramic powder dispersants. Our work aims to utilize these powerful dispersants in the use of dispersing  $\alpha$ - $\text{Si}_3\text{N}_4$  aqueous suspensions.

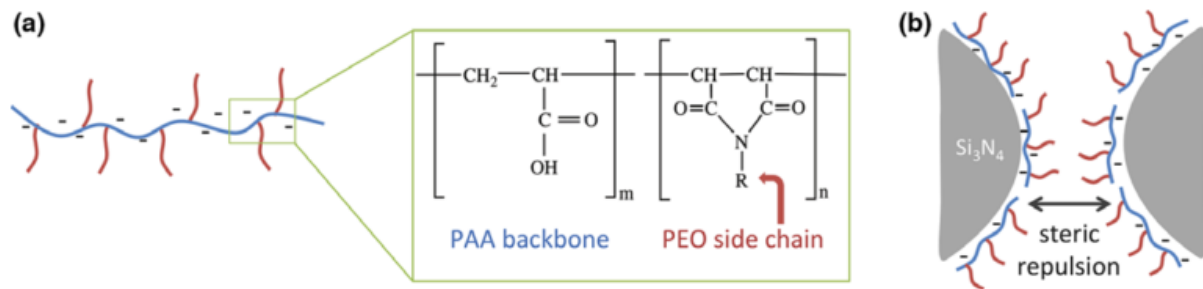


**Figure 1:** Schematic illustration of (a) molecular structure of typical comb polymer water-reducing admixtures composed of PAA backbones with PEO side chains ( $R = (\text{CH}_2\text{CH}_2\text{O})_x\text{-CH}_3$ ) and (b) coating of  $\text{Si}_3\text{N}_4$  particles with charged PAA backbone and PEO side chains providing steric repulsion between particles to stabilize the suspension (not drawn to scale).

Dispersion of  $\alpha$ - $\text{Si}_3\text{N}_4$  allows for the highest solids loading, which is pivotal for obtaining dense sintered parts. Silicon nitride has been difficult to disperse using traditional ceramic dispersion methods due to the unique surface chemistry. As-received silicon nitride powders contain a layer of silica on the surface less than a nanometer in thickness, which aid in the liquid-phase sintering processes by forming a silicate glass that is modified by ceramic powders added as sintering aids (such as yttria, alumina, and other rare-earth oxides). The surface silica contains silanol ( $\text{Si-OH}$ ) and secondary amine ( $\text{Si}_2\text{-NH}$ ) groups that can leach over time in an aqueous environment, altering the surface chemistry of the powders of the solution. Other research on producing aqueous silicon nitride suspensions has utilized calcination steps to form a thicker silica layer, and therefore more silanol surface groups, on the surface of the silicon nitride particles. While the increase of these silanol groups increase the particle's negative potential causing an electrostatic repulsion between particles, the increase in silica leads to less desirable high-temperature mechanical properties of sintered bodies since they contain more intergranular silica glass. Therefore, this steric repulsion imparted by the WRAs provides a more robust dispersion with the potential for more desirable mechanical properties of the sintered parts.

Zeta potential results (not shown) show no significant increase in the magnitude of zeta potential (a measure of electrostatic stabilization) between bare silicon nitride and silicon nitride with WRAs, implying the stabilization effect of WRAs is exclusively steric. When PAA alone is added to the silicon nitride powders, a large magnitude zeta potential increase is observed. This confirms that the PAA backbone of the WRA adsorbs to the surface of the silicon nitride, changing its effective surface charge.

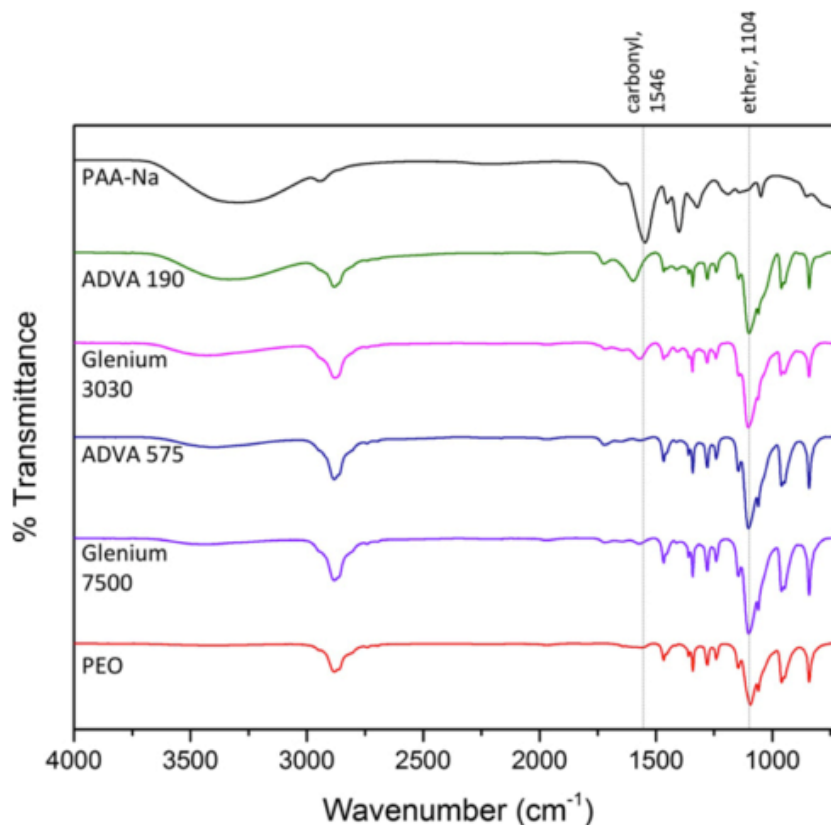


**Figure 2:** FTIR spectra of the four WRAs studied along with reference spectra for PEO and a sodium salt of PAA (PAA-Na). The strong peak around 1550 cm<sup>-1</sup> can be attributed to the C=O (carbonyl) stretch in PAA-Na, while the peak around 1100 cm<sup>-1</sup> can be assigned to the C–O–C (ether) stretching hydrating bond in PEO. The ratio of the area under these peaks is used to analyze the PAA- Na/PEO peak ratio.

Four different commercially available WRAs were used in this study: ADVA 190 and ADVA CAST 575 (WR Grace, Columbia, MD) as well as Glenium 7500 and Glenium 3030NS (BASF, Ludwigshafen, Germany). In order to determine the relative difference in chemical structure, FTIR spectra was taken for each WRA as well as reference spectra for (PEO) and a PAA sodium salt (PAA-Na). These results are presented in Figure 2. All samples show evidence of PEO and therefore likely have PEO side chains of varying molecular weights. Some samples have prominent PAA-Na peaks, indicating a backbone of PAA-Na.

In order to use WRAs as a silicon nitride dispersant they must be able to burn out cleanly in the nitrogen atmosphere employed during sintering of final silicon nitride parts. In order to insure clean burnout, thermogravimetric analysis (TGA) experiments were carried out in a nitrogen atmosphere for all of the WRAs studied (not shown). Results confirm all WRAs will burn out cleanly in a nitrogen atmosphere by 420 °C, validating their use in silicon nitride suspensions.

**Table I. Comb Polymer Dispersants Used To Stabilize Silicon Nitride Suspensions With Herschel–Bulkley Curve Fitting Parameters For Yield-Pseudoplastic Fluids**

Dispersant	PAA-Na/PEO Peak Ratio <sup>†</sup>	Sample Name	Amount of Si <sub>3</sub> N <sub>4</sub> /Y <sub>2</sub> O <sub>3</sub> /Al <sub>2</sub> O <sub>3</sub> powder (vol%)	Dispersant (vol%)	$\sigma_y$ (Pa)	$k$ (Pa·s <sup><i>n</i></sup> )	<i>n</i>
PAA-Na	1/0	PAA-Na-43-5	43	5	—	—	—
ADVA 190	0.67/1	A190-43-5	43	5	—	—	—
Glenium 3030 NS	0.27/1	G3030-43-5	43	5	22.3	11.7	0.56
		G3030-45-5	45	5	68.6	10.7	0.70
		<b>G3030-45-6</b>	45	6	78.1	15.3	0.77
ADVA CAST 575	0.12/1	A575-43-5	43	5	45.0	17.8	0.49
		<b>A575-45-3</b>	45	3	24.0	17.3	0.54
		A575-45-5	45	5	54.0	50.8	0.52
Glenium 7500	0.11/1	G7500-43-5	43	5	52.3	12.7	0.40
		<b>G7500-45-5</b>	45	5	54.5	11.8	0.69
		G7500-47-5	47	5	167.0	27.4	0.80
PEO	0/1	PEO-43-5	43	5	—	—	—

<sup>†</sup>Calculated via FTIR peak area ratios.

Bolded sample names refer to optimized dispersant contents at 45 vol% solid loading.

The highly-loaded suspensions made with each WRA are shown in Table I. Each suspension was made by gradually adding the ceramic powder to the water/WRA mixture and was mixed with a planetary mixer at high speeds to ensure thorough mixing. Three of the four WRAs, at a loading rate of 5 vol.% of the total suspensions, were able to produce suspensions with 43 vol.% solids loading, with one dispersant achieving up to 47 vol.%. This is a substantial increase over the use of a dispersant of PAA alone that was only able to stabilize up to 25 vol.% solids loading (our preliminary study with data not shown). While all suspensions exhibited a yield-pseudoplastic behavior, meaning they overcome a yield stress in order to flow at which point they decrease in viscosity with increased shear rate, some suspensions exhibited a transition to shear-thickening behavior at higher shear rates. Shear-thickening behavior corresponds to an increase in viscosity with increasing shear rate and is non-ideal for ceramic processing. Optimization of the three WRAs was conducted at 45 vol.% solids loading for ADVA 575 and Glenium 3030, while Glenium 7500 was optimized at 47 vol.%. The WRA content (in vol.% of the total suspension) was both increased and decreased from the starting 5 vol.% amount until the maximum shear rate at which shear-thickening was observed was obtained (data not shown). The optimized suspension formulations are bolded in Table 1, with rheology for the suspensions shown in Figure 3. ADVA 575 and Glenium 7500 are more ideal for ceramic processing since they exhibited no shear-thickening behavior in the shear rates studied, while Glenium 3030 transitioned to shear-thickening around 5 s<sup>-1</sup>.

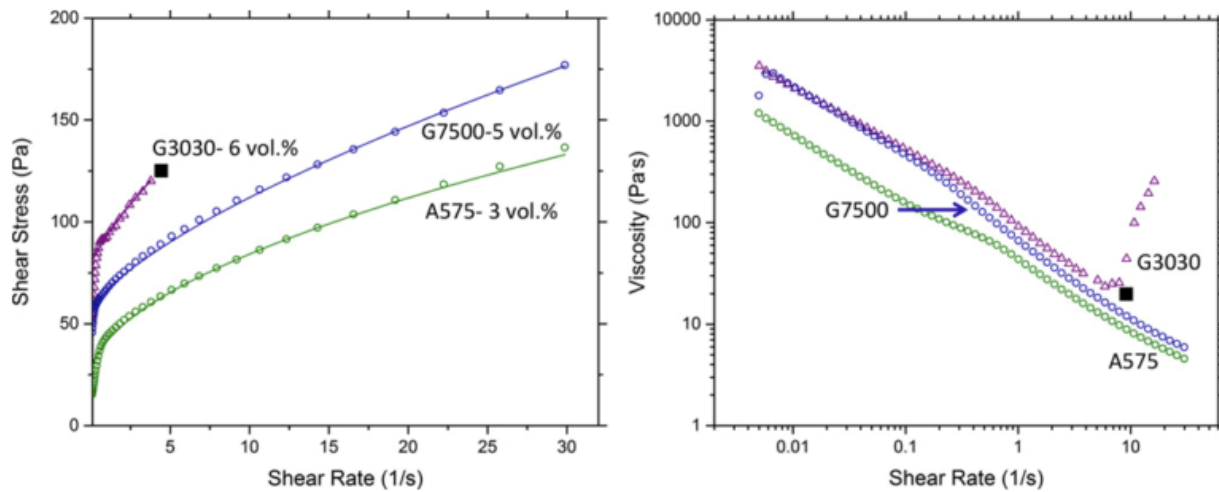


**Figure 3:** Flow curves for silicon nitride suspensions with 45 vol% solids loading and optimized dispersant amounts for the three studied dispersants. Curve fits to the Herschel–Bulkley fluid model are shown as solid lines with  $R^2 > 0.99$ . The critical shear stress is marked with a (■) for the G3030 sample, the only sample of the three exhibiting shear-thickening behavior. Viscosity as a function of shear rate also shows the G3030 sample has the highest viscosity, followed by G7500 and A575.

## ROOM-TEMPERATURE INJECTION MOLDING AND DIRECT WRITING OF AQUEOUS SILICON NITRIDE SUSPENSIONS

The two optimized WRA suspensions were used for room-temperature and low-pressure injection molding. Figure 4 shows the progression of the injection molding process. A 20cc syringe containing the suspension was connected to a plastic mold (made through a Form 1+ rapid prototyping machining) using an o-ring. A cylindrical MTS platen with a cross-head speed of 5 mm/min applied force to the top of the mold (centered with a ball bearing) in order to inject the suspension into the mold. Air vents at the end of the mold allow air to escape during molding to avoid porosity in the final part. The parts made via this injection molding process were removed within hours, with a green body shown in Figure 5A. The same billet after sintering in nitrogen atmosphere for 1 hr at 1750 °C is shown in Figure 5B. The sintered microstructure shown in Figure 5C shows high density as well as conversion to  $\beta$ - $\text{Si}_3\text{N}_4$  through the observation of elongated grains. Full conversion to  $\beta$ - $\text{Si}_3\text{N}_4$  was also confirmed via XRD analysis (not shown). The sintered parts had densities ranging from 95 – 97% TD, corresponding to 3 – 5% porosity present in the parts.

Preliminary additive manufacturing of these silicon nitride suspensions was completed using a Nscript SmartPump™ system, shown in Figure 6A. The system uses a syringe head that moves in the x,y, and z-axis with applied pneumatic pressure to deposit the suspension in a layer-by-layer fashion. An example of a 45 vol.% silicon nitride suspension deposited with a 0.61 mm syringe tip is shown in Figure 6B.

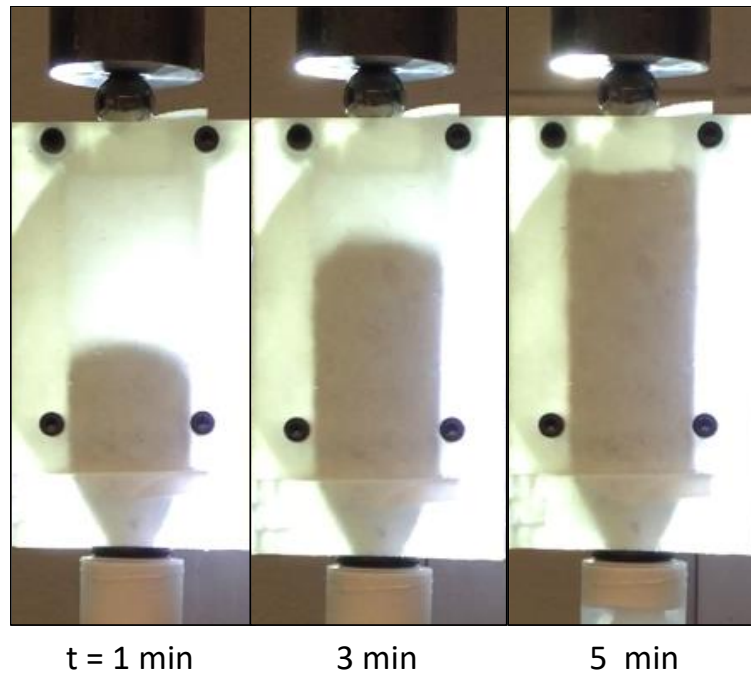


**Figure 4:** The evolution of silicon nitride aqueous suspension injecting into a clear plastic mold (made with a Form 1+ 3D printer) at room-temperature over time. The top MTS platen moves downward with a crosshead speed of 5 mm/min.

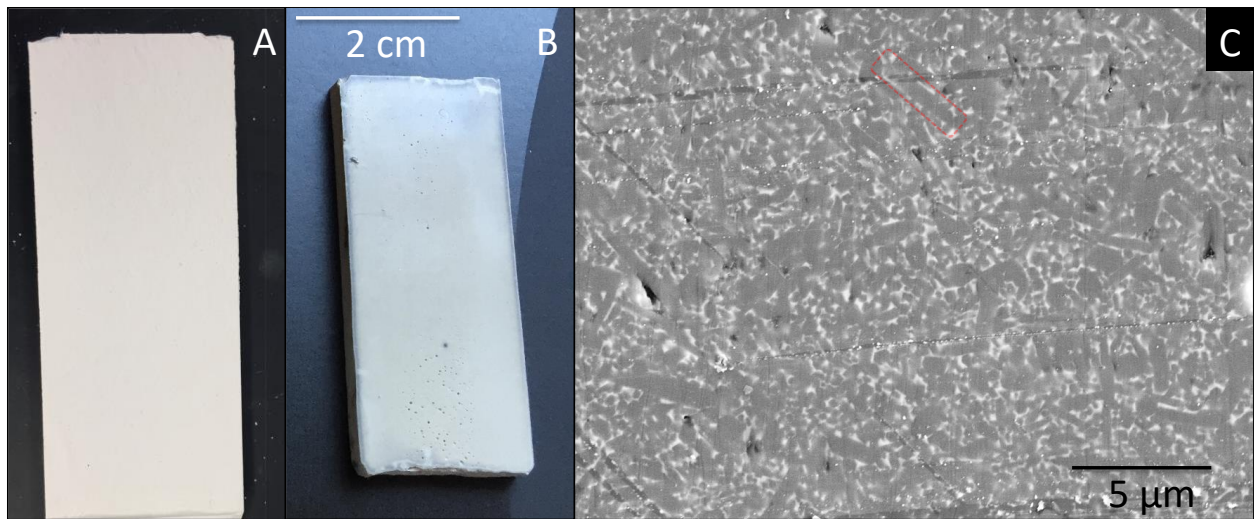


**Figure 5:** A) green body and B) sintered silicon nitride billet made via injection molding. C) A typical sintered microstructure with elongated  $\beta\text{-Si}_3\text{N}_4$  grains highlighted with a dashed red rectangle.

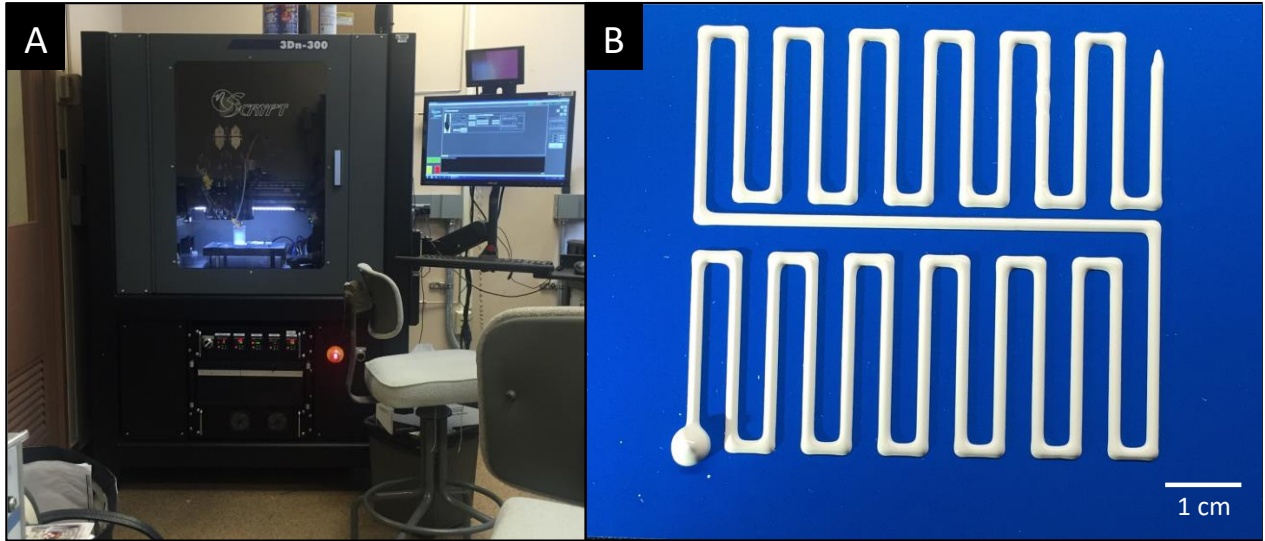


**Figure 6:** A) nScript 3d printer used at NASA Glenn Research Laboratory B) silicon nitride aqueous suspension deposited into a complex line pattern using the nScript.

## II. Additive Manufacturing of Dense Ceramic Parts via Direct Ink Writing of Aqueous Alumina Suspensions (Graduate Student: Lisa Rueschhoff, William Costakis Jr.)

### OVERVIEW OF WORK TO DATE

- Previously established aqueous alumina suspensions were applied to the direct ink writing additive manufacturing process to produce near-net shaped ceramic parts.
- Alumina suspensions were optimized for the direct ink writing process through changing the ceramic solids loading (51 – 58 vol.%) to tailor rheology. Wall slumping and layer uniformity were parameters used for the process optimization.
- Parts made from all suspensions were sintered to high density (~98% TD) with grain sizes ranging from 3.2 – 3.7  $\mu\text{m}$ . Flexural strength values ranged from 134 – 157 MPa and were not influenced by starting solids loading of the suspensions.
- Direct ink writing has been established as a viable process for producing near-net shaped ceramic parts starting with our highly-loaded aqueous suspensions.

Direct ink writing using a continuous filament will be explored in this study as a means to produce three-dimensional components using computer-controlled layer-by-layer deposition of a highly loaded colloidal suspension. This process was chosen for its ability to form near-net and complex shapes of easily densified ceramic parts due to the use of highly concentrated suspensions. The use of a low-cost syringe style 3D printer will be explored as a means to perform layer-by-layer deposition to form near-net-shaped ceramic parts. The syringe 3D printer used in this study is

shown in Figure 7A. Using a previously developed suspension formulation, ceramic suspensions composed of a ceramic powder, dispersant, polymer binder, and water can be utilized for direct writing complex ceramic objects. Alumina has been used in preliminary experiments as a model material due to its low cost, availability, and ease of densification. Figure 7B shows the deposition of an alumina suspension from a syringe nozzle tip with an inner diameter of 1.26 mm. Previous studies have optimized alumina suspensions using PVP as a binder and a cationic polyelectrolyte as a dispersant. These alumina suspensions show yield-pseudoplastic behavior, a term describing a material that is shear thinning after overcoming a yield stress. This behavior allows the suspensions to easily flow under the shear stress of deposition (after overcoming a yield stress) and to retain its shape once the stress is removed. This retention of shape allows multiple layers to be deposited on top of each other. The use of PVP will not only allow for more robust and machinable green bodies, but will also offer unique flow properties that can be more precisely tailored for this process. In this study, we have investigated the use and benefit of our tailored alumina suspensions in the direct writing process with the underlying design principle of maximizing solid loading while not compromising the quality of formed specimens. The suspensions studied are summarized in Table II.

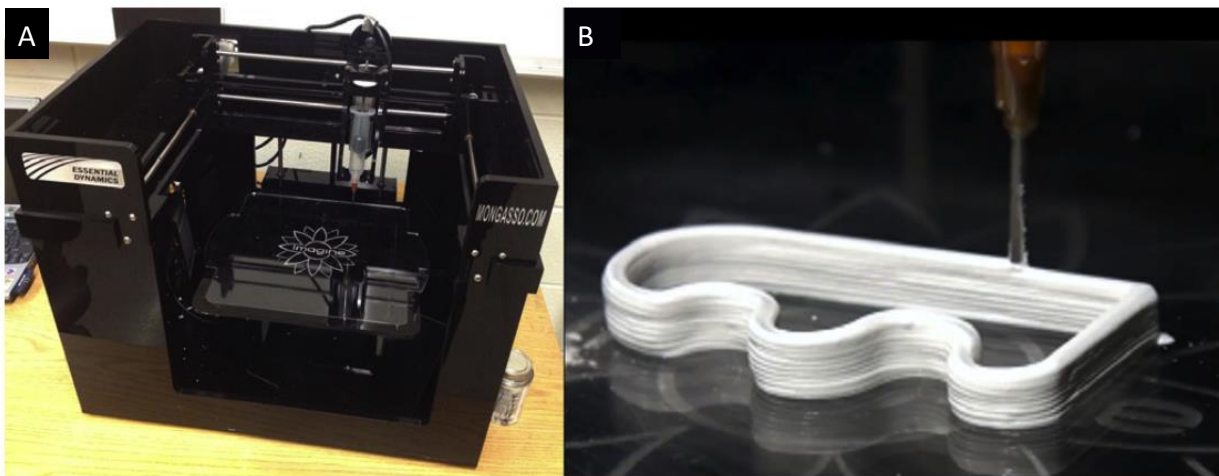


**Figure 7** A) Imagine syringe-style 3D printer from Essential Dynamics used for direct writing alumina suspensions. B) in progress deposition of a 55 vol.% alumina suspension layer by layer to form a test shape.

The maximum shear rate during deposition was determined using the following equation:

$$\dot{\gamma} = \frac{4Q}{\pi r^3}$$

Where  $Q$  is the volumetric flow rate during extrusion and  $r$  is the radius of the nozzle. Through this equation it was determined that the shear rate during extrusion ranged from  $19.5 \text{ s}^{-1}$  for a 56 vol.% alumina suspension to  $24.2 \text{ s}^{-1}$  for a 53 vol.% suspension. The stress as a function of shear rate flow curves, along with the viscosity as a function of shear rate, for the suspensions are shown in Figure 8A and Figure 8B, respectively. The flow curves obtained for each sample were fitted to the Herschel-Bulkley model for yield-pseudoplastic fluids<sup>15</sup> which is defined as:

$$\sigma = \sigma_y + k\dot{\gamma}^n$$

**Table II:** Compositions of Alumina-PVP Suspensions with Corresponding Herschel–Bulkley Curve Fitting Parameters for Yield-Pseudoplastic Fluids. Nominal Viscosity During Forming was Calculated Based on Measured Shear Rates During Forming for Each Suspension, and Average Layer Height was Measured from Green Body Specimens Formed via Direct Writing

$\text{Al}_2\text{O}_3$ (vol.%)	Dispersant (vol.%)	PVP			$n$	Nominal viscosity during forming (Pa·s)	Average deposited layer height (mm)
		MW = 55k (vol.%)	$\sigma_y$ (Pa)	$k$ (Pa·s <sup><math>n</math></sup> )			
51	4.5	5.3	83	16.7	0.57	7.5	$0.88 \pm 0.37$
53	4.4	5.1	116	17.6	0.61	9.9	$0.85 \pm 0.14$
55	4.2	4.9	157	18.7	0.64	12.8	$0.85 \pm 0.07$
56	4.1	4.8	191	27.6	0.56	17.2	$0.90 \pm 0.20$
58	3.9	4.5	268	19.7	0.68	25.0	$0.86 \pm 0.32$

Where  $\sigma$  is the shear stress,  $\sigma_y$  is the yield stress for the material,  $k$  is the consistency index,  $\dot{\gamma}$  is the applied shear rate on the material, and  $n$  is the flow index that ranges from 0 to 1. A material is considered shear-thinning if the flow index is less than 1. The shear stress during deposition for each suspension, using the equation listed above, is denoted on the graphs in Figure 8 with a “x”. The suspension with the highest solid loading, 58 vol.% alumina, had the highest yield was the most difficult suspension to extrude as the syringe tip would dry and clog easily, while the 51 vol.% alumina suspension could flow easily from the syringe, but did not support each subsequent deposited layer well. Therefore, the 53, 55, and 56 vol.% suspensions were optimal for direct writing as they flowed easily from the syringe and were viscous enough to support multiple deposited layers of complex structures. The layer uniformity, shown in Table II, was also the most consistent (lowest standard deviation) for specimens printed with these suspensions.

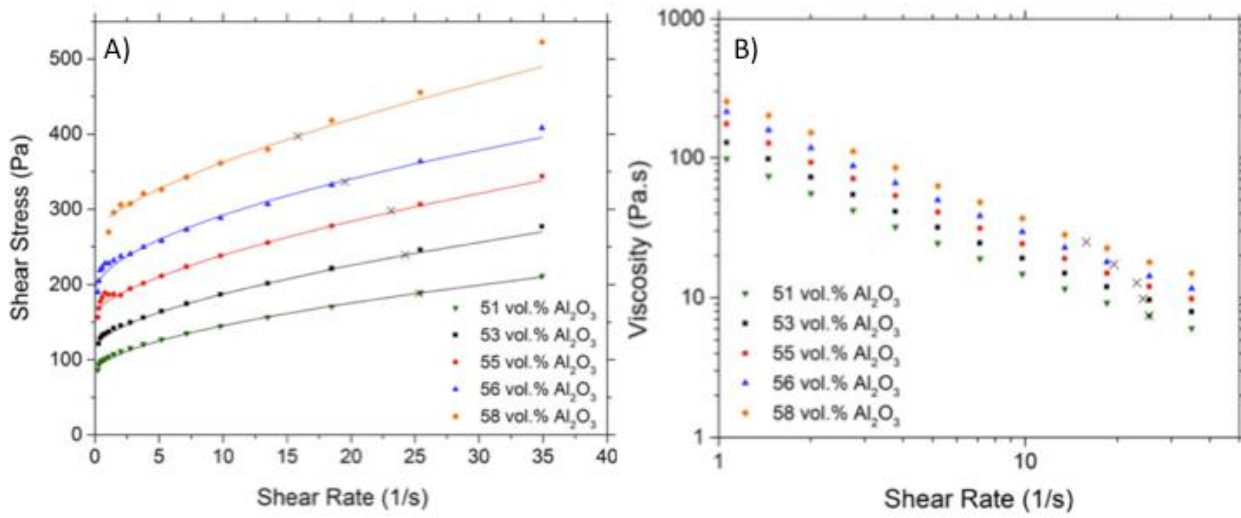


**Figure 8:** A) Flow curves for alumina suspensions with varying solids loading. Solid lines correspond to fit to the Herschel-Bulkley model ( $R^2 > 0.98$ ). The 51 and 58 vol.% alumina rheology was found unsuitable for direct writing. An "x" denotes the nominal shear stress during extrusion for each suspension based on shear rate calculations. B) Log viscosity against log shear rate plots of the same alumina suspensions.

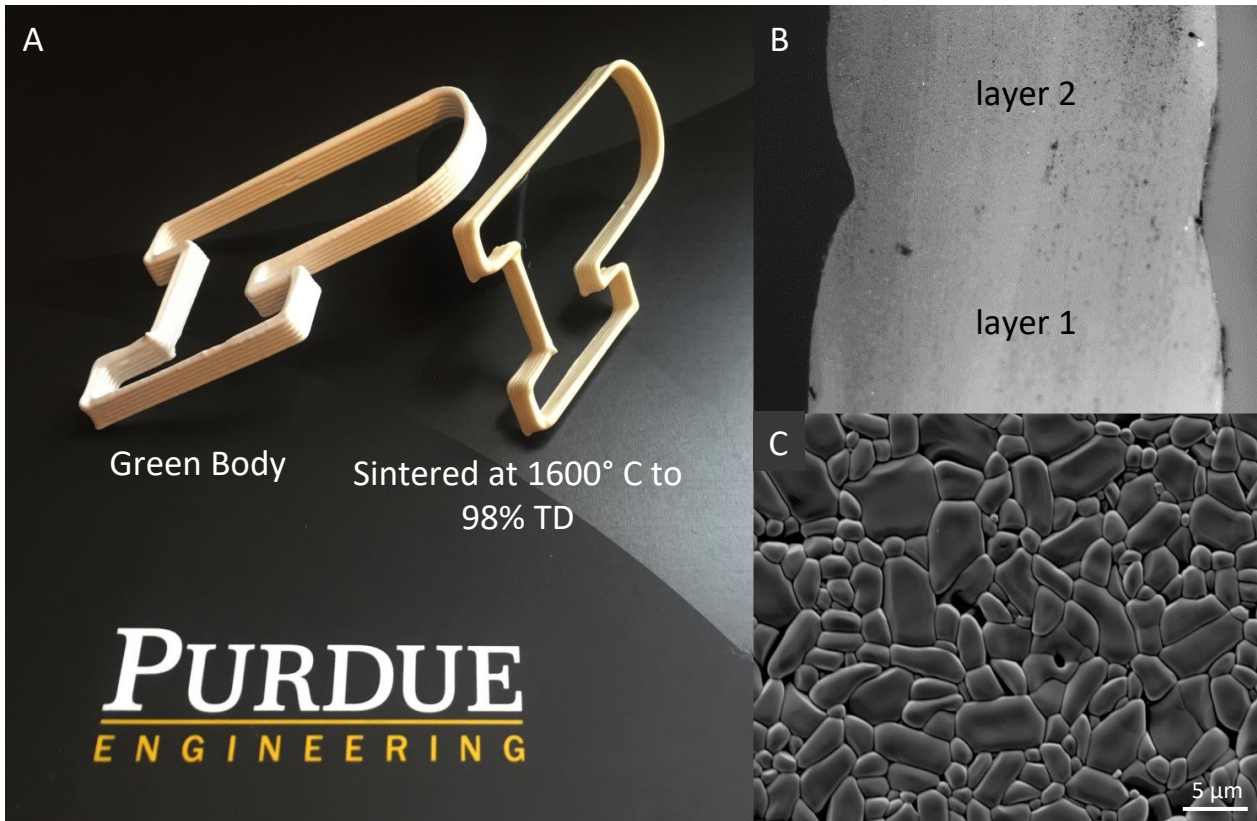


**Figure 9:** A) green body and sintered specimens produced via direct writing of a 55 vol.% alumina suspension. B) A cross-section of a sintered specimen showing no delamination, cracking, or porosity between layers. C) A typical sintered microstructure with small amounts of porosity observed most often on grain boundaries.

Figure 9A shows an example of a Purdue “P” made via direct ink writing of the alumina suspensions. The cross section of the sintered part in Figure 9B shows strong adhesion between deposited layers, with no delamination, cracking, or porosity observed.

Table III shows the calculated sintered bulk density, average grain size, and average flexural strength of the sintered parts. The calculated values for average flexural strength, were determined using ASTM C1161 for samples formed via direct writing 53, 55, and 56 vol.% alumina suspensions into size B bend bars.

**Table III:** Average Sintered Bulk Density, Average Grain Size, and Average Flexural Strength for Sintered Samples Made Through Direct Writing Alumina Suspensions

$\text{Al}_2\text{O}_3$ (vol.%)	Average Sintered Bulk Density ( $\text{g}/\text{cm}^3$ ) [%TD]	Average Grain Size ( $\mu\text{m}$ )	Average Flexural Strength (MPa)
51	N/A	N/A	N/A
53	$3.90 \pm 0.03$ [98.1]	$3.49 \pm 0.44$	$147.5 \pm 11.2$
55	$3.90 \pm 0.01$ [98.0]	$3.17 \pm 0.37$	$156.6 \pm 17.5$
56	$3.91 \pm 0.01$ [98.2]	$3.71 \pm 0.37$	$133.6 \pm 17.8$
58	N/A	N/A	N/A

Average flexural strengths were lower than expected but were determined to be largely effected by the porosity introduced during mixing of the aqueous suspensions. The etched micrographs confirmed very little porosity in grains and at grain boundaries due to incomplete sintering, and fracture surfaces show no delamination or preferential cracking between deposited layers. There was no relevant difference found in the material properties (e.g., density and grain size) and mechanical properties with respect to solid loading. Future work will include evaluating alternate mixing approaches for the suspensions and methods of loading syringes to obtain more uniformly mixed suspensions and therefore parts with improved properties. This unique direct writing process that takes advantage of the room-temperature flow properties, along with green body strength, of these suspensions will be investigated as a technique for fabricating more complex geometries ranging from overhanging structures to ceramic matrix composites using two-phase suspensions or two separate ceramic suspensions.

**III. Additive Manufacturing Of Boron Carbide Via Continuous Filament Direct Ink Writing Of Aqueous Ceramic Suspensions (Undergraduate/Graduate Research: William Costakis Jr, Graduate Student Support: Andres Diaz-Cano, Lisa Rueschhoff)**

**OVERVIEW OF WORK TO DATE**

- Demonstrated that an additive manufacturing technique (direct ink writing) could be used to fabricate near-net shaped  $\text{B}_4\text{C}$  components at room temperature with aqueous suspensions

- Explored the effects of dispersant polyethylenimine (PEI) polymer molecular weight (25,000 and 750,000 g/mol) and B<sub>4</sub>C solids loading (48 to 56 vol.%) on the rheological properties and final quality of specimens
- Observed that an increase in the molecular weight of the polymer dispersant led to an increase in the rheological properties (yield stress, viscosity, storage shear modulus) and final specimen layer shape retention and warpage.
- An increase in the rheological properties of the suspensions correlated to increased layer shape retention and the ability to support additional layers.
- Minimized warpage effects through use of a low molecular weight polymer and reduction of the B<sub>4</sub>C solids loading.
- Found that the 54 vol.% B<sub>4</sub>C suspension with a PEI molecular weight of 25k g/mol was optimum for direct writing because of the high filament layer shape retention and zero warpage displacement during drying.

Filament direct ink writing is an additive manufacturing technique that can produce near-net ceramic structures at room temperature. Based on previous success with alumina, it was proposed that this direct writing technology can be used with aqueous boron carbide suspension. The combination of the physical properties of boron carbide (low density, high melting point, low chemical reactivity, and high hardness) and the cost effective nature of room temperature direct ink writing and pressureless sintering make this method ideal for armor applications.

Previous by a Andres Diaz showed that PEI, a cationic polyelectrolyte dispersant, had a high electrostatic potential with B<sub>4</sub>C allowing for the stabilization of ceramic powders and suspensions with desirable flow properties. The suspensions formulated for the current study are a mixture of 48 to 56 vol.% B<sub>4</sub>C, 5 vol.% (PEI) polymer dispersant, 5 vol.% hydrochloric acid (HCl), and a balance of water. The B<sub>4</sub>C solids loading and water content were systematically altered to determine the optimal rheological properties for forming and are shown in Table IV. It is important to note that all B<sub>4</sub>C powders were attrition milled with tungsten carbide (WC) and as a result 2.7 vol.% residual WC was introduced to the system.

Flow curves demonstrating the dependence of shear stress on applied shear rate for the B<sub>4</sub>C suspensions are shown in Figure 10 for PEI molecular weights of a) 25k g/mol and b) 750k g/mol. These flow curves reveal that all suspensions behaved in a yield-pseudoplastic manner with shear-thinning behavior. Yield-pseudoplastic suspensions are ideal for continuous direct writing as they will flow in a shear thinning manner after an applied shear stress exceeds the yield stress and retain the formed shape while supporting other deposited layers after extrusion. It was found that an increase in the B<sub>4</sub>C solids loading and PEI molecular weight led to an increase in the yield stress ( $\sigma_y$ ).

Plots of storage shear modulus versus oscillation stress for the B<sub>4</sub>C suspensions as a function of PEI molecular weight are shown in Figure 11a (25k g/mol) and b (750k g/mol). Each suspension displayed an equilibrium modulus ( $G'_{eq}$ ) within the linear viscoelastic region. Values for each suspension are reported in Table IV. It was found that an increase in the B<sub>4</sub>C solids loading and/or PEI molecular weight led to an increase in the equilibrium modulus, indicating an increase in gel strength.

**Table IV.** Compositions of B<sub>4</sub>C suspensions with corresponding Herchel-Bulkley curve fitting parameters for yield-pseudoplastic fluids. The equilibrium storage modulus is provided. Warpage displacement (X) is the measurement from a flat surface to the bottom of the B<sub>4</sub>C green body specimen at the maximum point of displacement. Average layer height is the averaged cross sectional height (Y) of individual green body filament layers. The optimum suspension is shown in bold. An (\*) denotes samples with estimated Herchel-Bulkley fit parameters due to low statistical measurements ( $R^2 < 0.95$ ).

PEI Molecular Weight [g/mol]	B <sub>4</sub> C [vol.%]	Water [vol.%]	$\sigma_y$ [Pa]	$k$ [Pa·s <sup>n</sup> ]	n	G' <sub>eq</sub> [Pa]	Warpage Displacement [mm]	Average Layer Height [mm]
25,000	50	40	24	11.6	0.44	64	0.0	-
25,000	52	38	37	22.3	0.46	274	0.0	-
<b>25,000</b>	<b>54</b>	<b>36</b>	<b>122</b>	<b>51.3</b>	<b>0.46</b>	<b>962</b>	<b>0.0</b>	<b>0.79 +/- 0.07</b>
25,000	56	34	359*	66.5*	0.47*	3418	0.8	0.85 +/- 0.05
750,000	48	42	20	14.6	0.38	155	0.0	-
750,000	50	40	43	15.3	0.42	767	1.25	0.67 +/- 0.12
750,000	52	38	83	55.4	0.36	1844	2.75	0.73 +/- 0.08
750,000	54	36	352*	108.9*	0.25*	3760	4.50	0.76 +/- 0.04

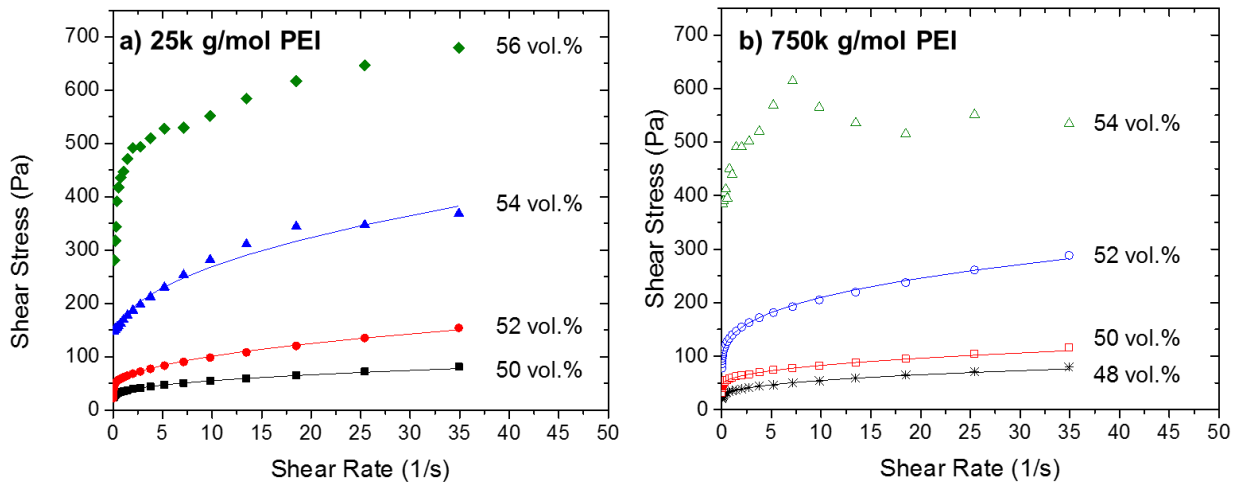


**Figure 10:** Flow curves of varying B<sub>4</sub>C suspensions with a) 25k g/mol and b) 750k g/mol PEI molecular weight. Solid lines correspond to a fit of the Herschel-Bulkley fluid model with fitting parameters ( $R^2 > 0.98$ ) for each data set shown in Table 1. An increase in solids loading and polymer molecular weight both led to higher yield stresses.

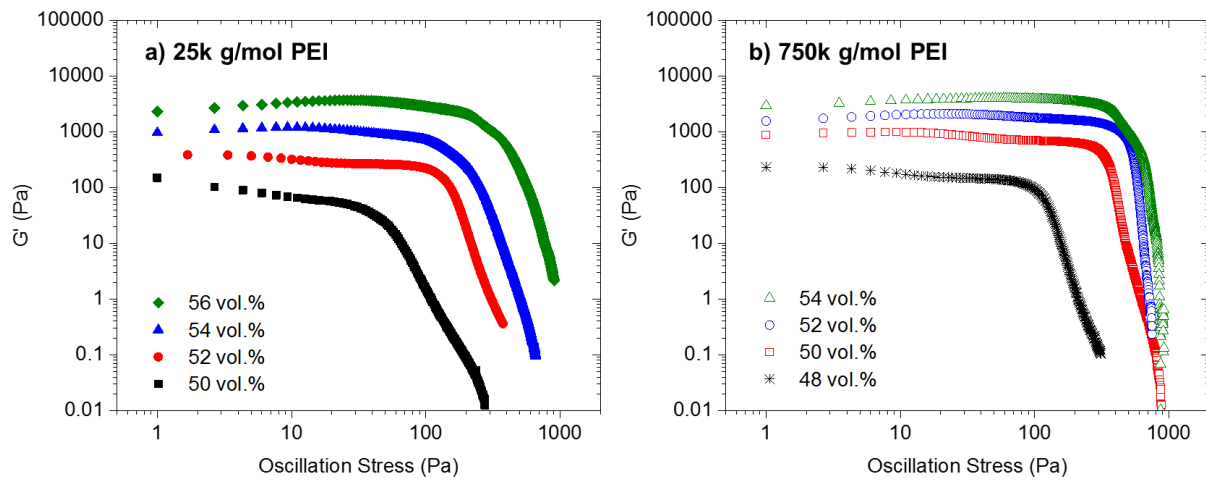


**Figure 11.** Log storage modulus ( $G'$ ) vs log oscillation stress plots obtained at a frequency of 1Hz of varying B<sub>4</sub>C suspensions with a) 25k g/mol PEI and b) 750k g/mol PEI molecular weight. Increasing the B<sub>4</sub>C solid loading and polymer molecular weight resulted in an increase in gel strength ( $G'_{eq}$ ).

Final quality of formed specimens based on filament layer shape retention and warpage upon drying was assessed. Specimen shape retention was quantified by measuring the average filament layer height in cross sectional images of green body specimens shown in Figure 12. The degree of warpage was taken to be the measurement from a flat surface to the bottom of the B<sub>4</sub>C specimen at the maximum point of displacement, as shown in Figure 13. The summaries of measurements for average filament layer height and warpage displacement (X) are shown in Table IV. The specimen shape retention was found to directly correlate with the suspension yield stress and equilibrium storage modulus. In general, suspensions made with PEI 750k g/mol molecular weight

possessed higher shape retention than suspensions made with PEI 25k g/mol molecular weight for the same solids loading.

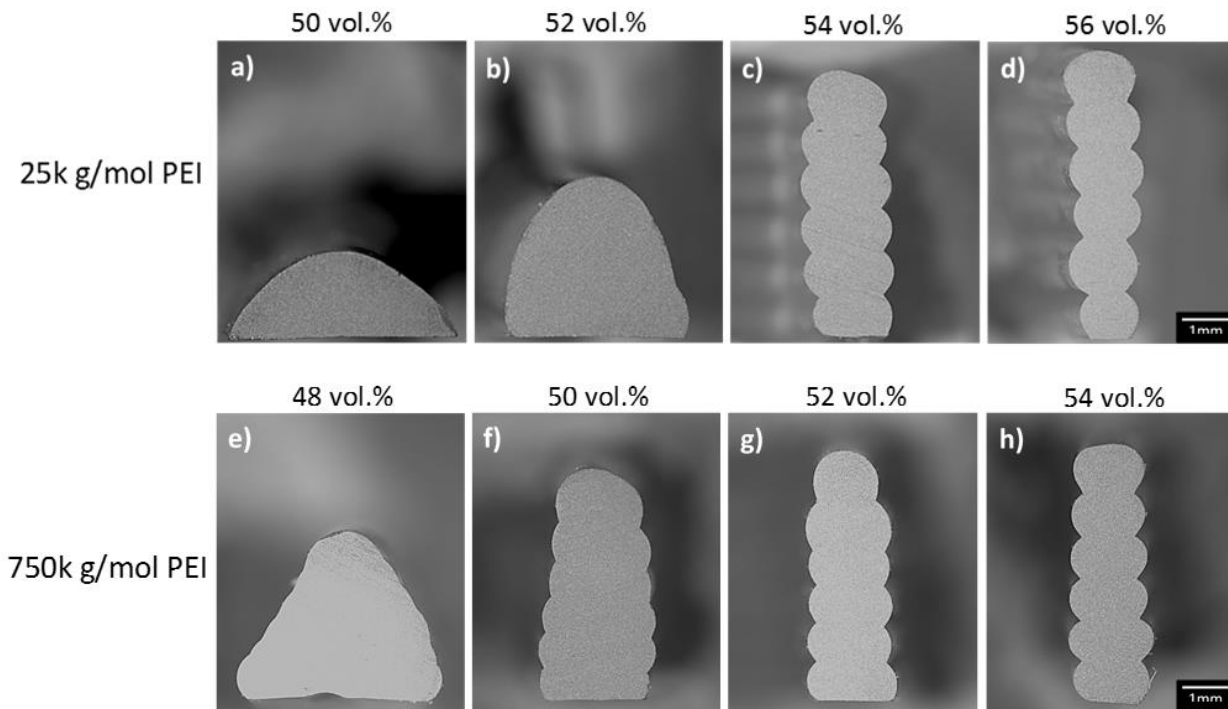


**Figure 12:** Cross sectional comparison of green body specimen filament layer heights formed via direct ink writing with varied polymer molecular weight and B<sub>4</sub>C solids loading.

During the drying process, shrinkage induced warpage effects reduced the final specimen quality. The amount of warpage of each specimen can be seen in the profile images shown in Figure 13, with warpage displacement values for each shown in Table IV. It was found that an increase in molecular weight of PEI led to an increase in the amount of warpage for suspensions that had sufficient strength to retain a filament shape.

It was determined that the 54 vol.% B<sub>4</sub>C suspension with a PEI molecular weight of 25k g/mol produced the highest final quality specimens. Specimens produced with this suspension showed no green body warpage displacement and had adequate strength to retain shape due to its yield stress of 122 Pa and elastic storage modulus of 962 Pa. A final sintered sample formed with this suspension is shown in Figure 14a, with a cross sectional and profile view shown in Figure 14b and 14c, respectively. The cross sectional and profile views of the sintered specimen show adhesion between each printed layer with no systematic residual porosity associated with the forming process for this particular suspension.

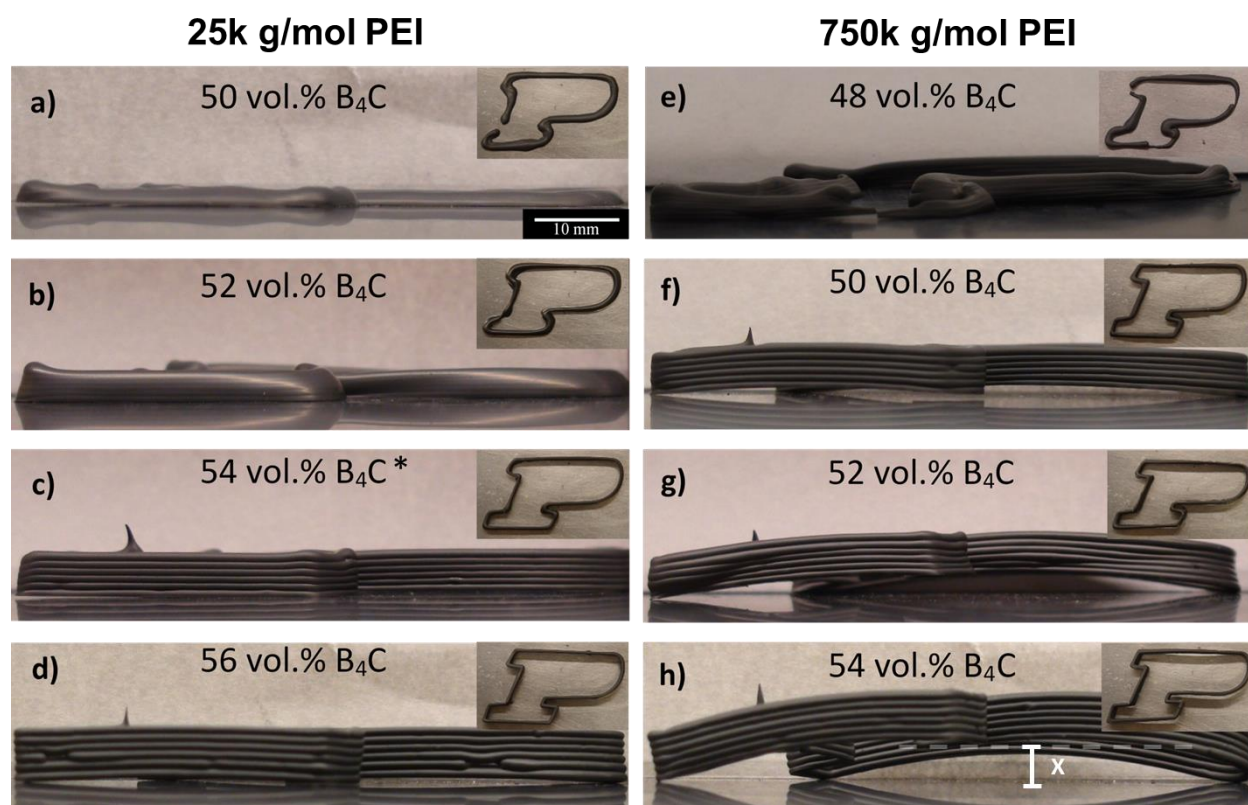


**Figure 13.** Profile comparison of samples formed via direct ink writing with varied polymer molecular weight and B<sub>4</sub>C solids loading. The inset figure shows the top views of the Purdue “P” and the scale for this image is 5 times smaller than the profile image. Warpage displacement (X) is the measurement from a flat surface to the bottom of the B<sub>4</sub>C structure at the maximum point of displacement and is illustrated in image h).

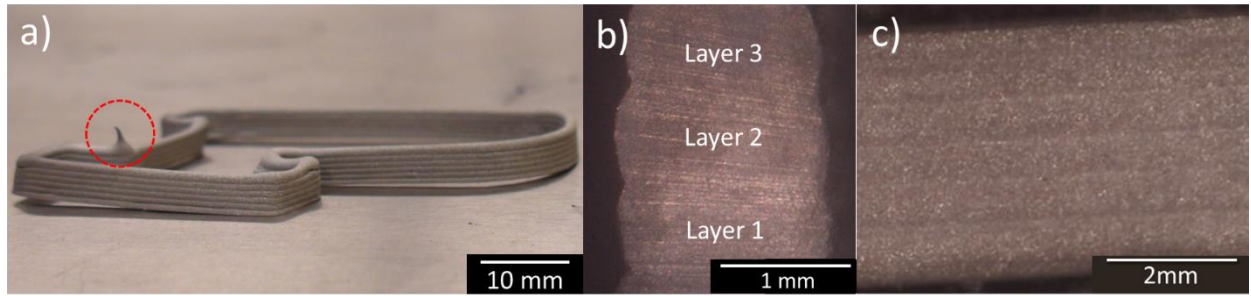


**Figure 14.** a) Sintered sample formed via direct writing a suspension with 54 vol.% B<sub>4</sub>C and 25k g/mol PEI. A dashed circle indicates the starting and stopping point for each layer. b) A cross sectional and c) profile view of the sintered piece show adhesion between each printed layer.

#### **IV. Alumina Injection Molding with IP Optioned by Masten Space Systems.**

Masten Space Systems an aerospace manufacturer startup company currently located in Mojave, California is interested in using the developed room-temperature injection molding process to make cost effective ceramic turbine blade. A three dimensional CAD drawing of the supplied polymer mold is shown in Figure 15a. Based on previous success with alumina (Valerie), zirconium diboride (Valerie), boron carbide (Andres), and silicon nitride (Lisa) it was proposed that room-temperature injection molding of aqueous ceramic suspensions can be used to develop complex shaped (turbine) high temperature ceramic structures. Alumina was selected as a test material to develop the proof of concept due to the ease of use, low cost and optimized rheological properties. Due to the complex nature of the selected mold, the dried suspensions would need a higher green body strength when compared to previous studies. It was determined that a 51 vol.% Al<sub>2</sub>O<sub>3</sub> suspension with 5 vol.% PVP produced the highest final quality specimens. An image of the injection process is shown in Figure 1b. High density alumina turbine blades were successful injection molded. An image of the final product is shown in Figure. 16. In order to reduce drying induce cracking and promote successful removal of the green sample, filter paper was applied to the surface of the mold. Future, work will consist of developing a mold releasing agent that allows for the deconstruction of the mold during the drying process. This is important so that the piece can shrink freely during the drying process.

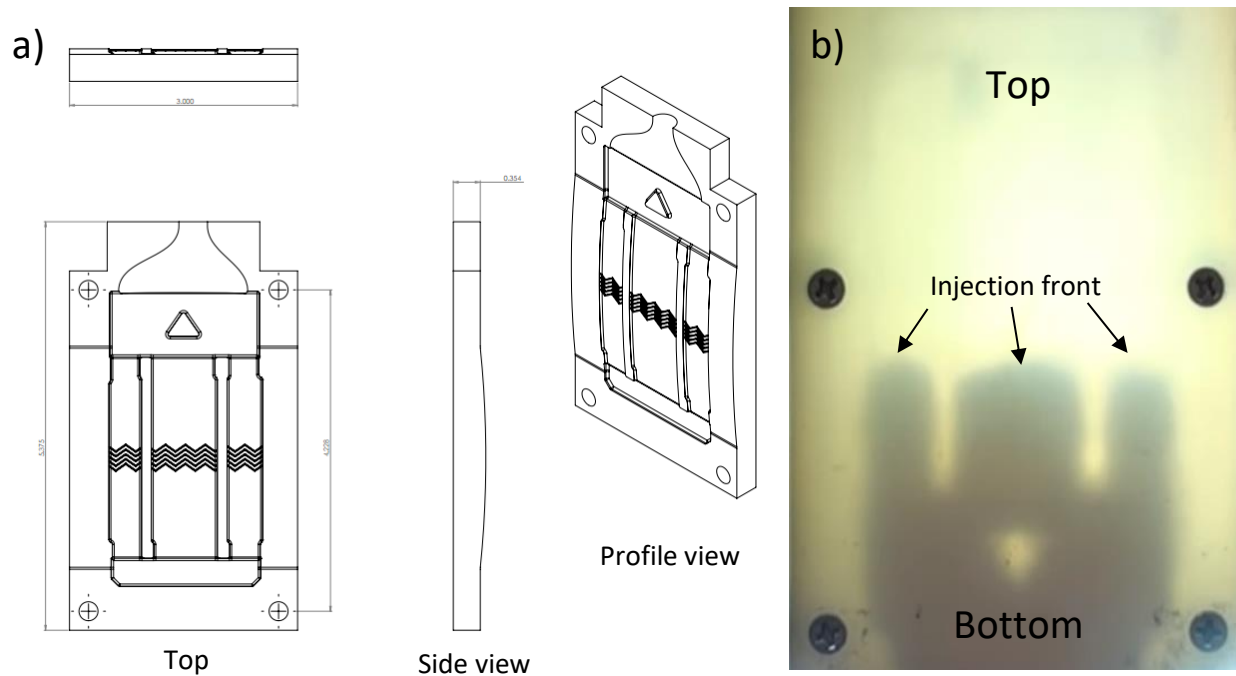


**Figure 15.** a) Blue print of the 3D printed mold. b) An image of the mold being injected with the alumina suspension. The injection front is labeled to illustrate how the mold was filled. The mold cavity was injected from the bottom to top with a simple syringe.



**Figure 16.** Sintered sample formed via injection molding of a suspension with 51 vol.%  $\text{Al}_2\text{O}_3$  with 5 vol.% PVP.

## V. Boron Carbide Stabilization and Sintering Investigations (Graduate Student: Andres Diaz Cano)

Boron carbide is one of the hardest known materials, with values around 35 GPa possible. Additionally, its low density of 2.52 g/cm<sup>3</sup> is desirable for armor. With a melting point of ~2450°C it is also utilized in severe chemical environments over wide temperature ranges. Boron carbide components are normally produced via hot pressing or spark plasma sintering. Although components have been successfully made, geometries are limited to plates, bars, or disks. Near-net shape forming methods, to include traditional injection molding, afford production of complex-shaped components. However, large amounts of volume are typically required, along with high processing pressures and temperatures.

The present work aims to develop processing methods where complex-shaped B<sub>4</sub>C components can be formed at room temperature using minimal binder contents and processing pressures. In our approach, water-based suspensions with above 50 vol% B<sub>4</sub>C and binder concentrations below 5 vol% are employed. The rheological properties of the suspension are tailored for each forming process to include injection molding, casting, and additive manufacturing.

Furthermore, an investigation of sintering aids for B<sub>4</sub>C was attempted to lower the sintering temperature to below 2000°C. Ultimately, B<sub>4</sub>C suspensions with the best combination of sintering aid will be injection molded, sintered, and characterized. Density, hardness, and flexural strength are among the properties that will be studied.

### OVERVIEW OF WORK TO DATE

- Highly loaded suspension of boron carbide have been prepared using polyethylenimine (PEI) as dispersant. Suspensions with up to 56 vol% B<sub>4</sub>C, with less than 5 vol% PEI, have been developed.
- The suspension formulations have been modified to tailor their rheological properties. The yield stresses of the suspensions have been modified by changing dispersant and/or ceramic concentrations. Boron carbide suspensions have been successfully used for injection molding, casting, and additive manufacturing.
- The effect of sintering aid type and amount on the density of pressureless sintered boron carbide was performed using dry-pressed pellets. Samples with the highest values of density and hardness were characterized. The effect of the B<sub>4</sub>C powder surface on sintering have also been investigated.

Preparation of high ceramic solids loading requires an understanding of the inter-particle forces obtained via zeta potential experiments. The zeta potential of boron carbide zeta as a function of the dispersant type and pH of the solution are shown in Figure 17. Four different dispersants were investigated to determine which one would be best to produce stable suspensions with the greatest vol.% of B<sub>4</sub>C. The four suspensions are indicated in the legend associated with Figure 17. The PEI

dispersant had a weight average molecular weight of 25,000 g/mol.

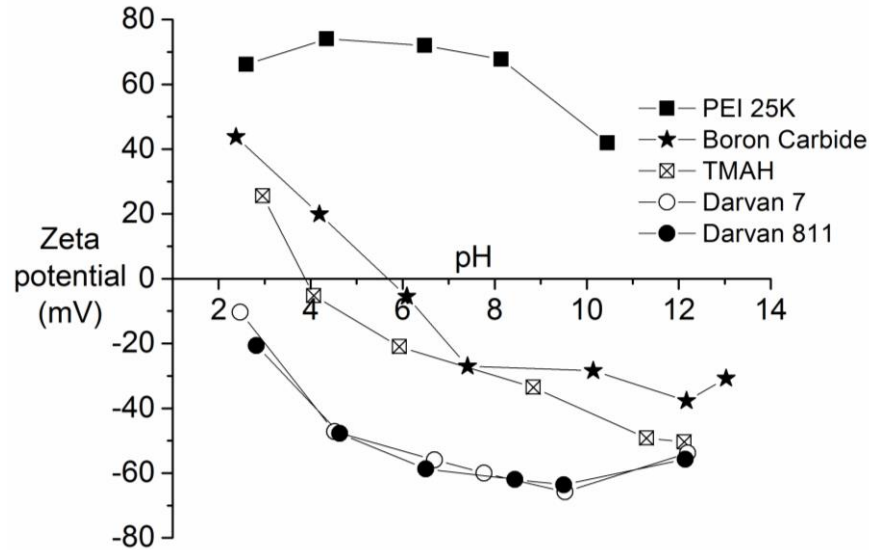


**Figure 17.** Zeta potential values as function of pH for common dispersants used for boron carbide. Hydrochloric acid (HCl) and sodium hydroxide (NaOH) were used to change the suspension pH. Isoelectric point of boron carbide corresponded to a pH between 5 and 6.

The isoelectric point of boron carbide powder (no dispersants) is between 5 and 6. In terms of absolute value of zeta potential, the PEI with molecular weight of 25k, Darvan 7 and Darvan 811 all displayed comparable results. Darvan 7 and Darvan 811 showed a maximum zeta potential with B<sub>4</sub>C powders at a pH of 9.5 of -63.8 mV and -63.6 mV, respectively. PEI and B<sub>4</sub>C exhibited a maximum zeta potential of 74 mV at a pH of 4.3. Thus, based on zeta potential results alone, it would be expected that Darvan 7, Darvan 811, and PEI should all afford preparation of highly loaded suspensions of B<sub>4</sub>C.

These dispersants were used to form boron carbide suspensions and the flow behavior was analyzed. Concentrations of 40 Vol % B<sub>4</sub>C and 5 Vol% dispersant were used for initial rheological tests. Figure 18 shows the change in viscosity as a function of applied shear rates for a range of 0.01s<sup>-1</sup> to 35 s<sup>-1</sup>. Although PEI 25k, Darvan 7, and Darvan 811 had comparable absolute values of zeta potentials, their flow behavior was different. Suspensions made with Darvan 7 and Darvan 811 displayed Bingham fluid rheological behavior, i.e. their viscosity increased linearly after the shear yield stress was overcome. Bingham fluids will also have higher viscosities compared to yield pseudo-plastic fluids at the same shear rates. This makes Darvan 811 and Darvan 7 a poor dispersant choice for preparing highly-loaded boron carbide suspensions. On the other hand, PEI 25k displayed significantly lower viscosity and more uniform behavior as shear rate was increased.

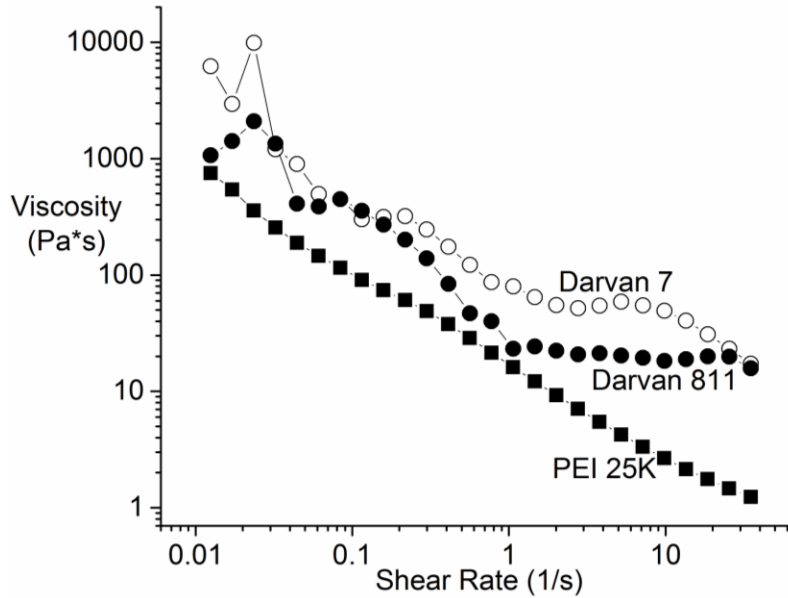


**Figure 18.** Rheological behavior of 40 vol. % boron carbide suspensions with 5 vol. % dispersant. Dispersants with comparable electrostatic effects showed different flow behavior. PEI 25k showed the lowest viscosities and uniform shear-thinning behavior.

Once PEI was selected as the dispersant for boron carbide, different molecular weights were evaluated to study their effect on suspension stability. The molecular weights of PEI studied included: 1300 g/mol (1.3k), 25000 g/mol (25k), 750000 g/mol (750k), and 2000000 g/mol (2000k).

When mixed with B<sub>4</sub>C powders, the PEI molecular weights of 1.3 K and 2000k (not shown) demonstrated lower zeta potential, in addition to higher viscosities, compared to PEI with molecular weight of 25k and 750 k. PEI molecular weights of 25k and 750k, respectively, showed a maximum zeta potential of 74mV at a pH of 4.3 and 75.9 mV at pH of 6.5, respectively. Based on these results, PEI 25k and 750k were expected to efficiently stabilize boron carbide suspensions.

Both molecular weights were used to form boron carbide suspensions with 50 vol.% B<sub>4</sub>C powder and 5 vol.% PEI. The viscosity versus shear rate behavior is shown in Figure 19. PEI with either molecular weights demonstrated uniform flow behavior without abrupt changes in viscosity, suggesting that it is possible to form stable suspensions using either dispersant. However, B<sub>4</sub>C suspensions made with PEI 25k dispersant demonstrated lower viscosities. Therefore, 25k PEI was chosen as the best possible dispersant to make highly loaded (>50 vol% B<sub>4</sub>C) suspensions.

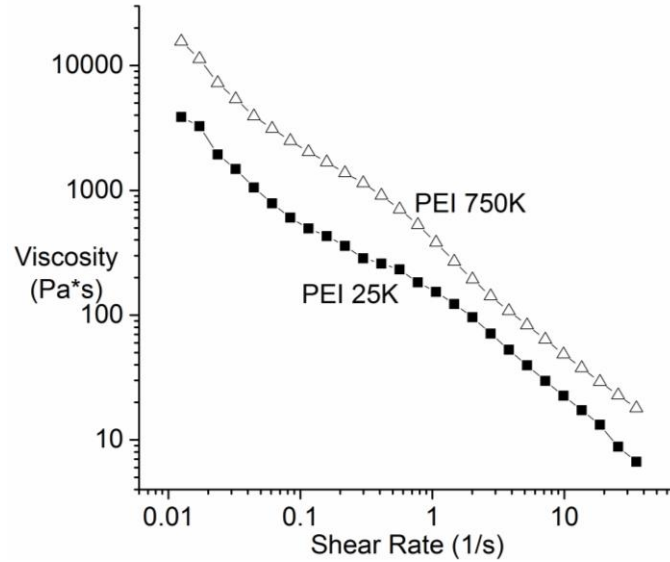


**Figure 19.** Flow curves for PEI 25k and 75k. Boron carbide concentration of 50 vol.% with 5 vol. % dispersant. PEI 25k had lower viscosity.

All the rheological studies performed previously used 5 vol% 25k PEI without considering whether this was the optimum amount to add. Thus, B<sub>4</sub>C suspensions were made with different amounts of PEI 25k added (2.5, 3.5, 5, 7.5, and 10 vol.%) to determine the optimum concentration. Boron carbide concentration was held constant at 50 vol.% for all suspensions and viscosities were compared at a shear rate of 10 s<sup>-1</sup>. A concentration of 3.5 vol. % yielded the lowest viscosity. Lower and higher PEI contents resulted in suspensions with higher viscosity. Based on the specific surface area of B<sub>4</sub>C obtained from BET analysis, a PEI concentration of 1.83 mg/m<sup>2</sup> was determined as the optimal amount to produce boron carbide suspensions at concentrations of greater than 50 vol. %. As shown in Figure 20, suspensions with up to 56 vol% B<sub>4</sub>C powder loadings have been achieved.

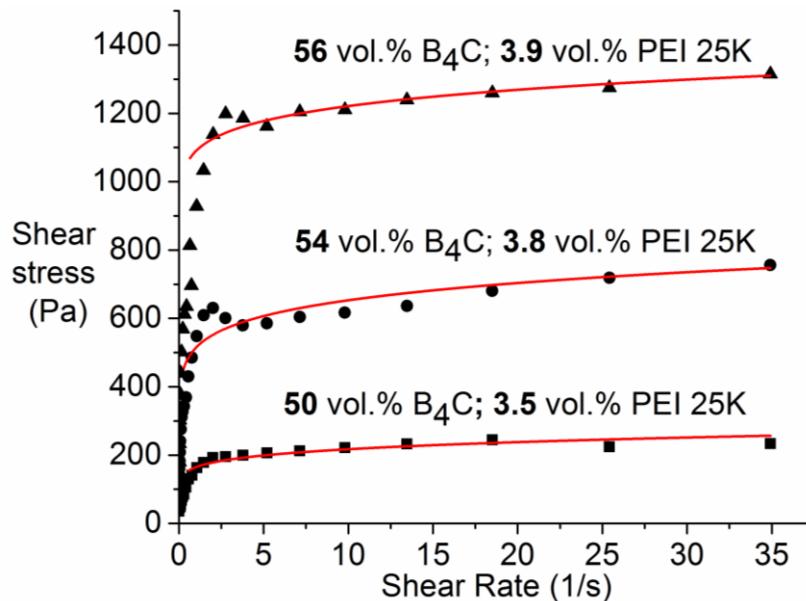


**Figure 20.** Shear stresses as function of applied shear rates. Flow curves of boron carbide suspensions using an optimal PEI content of 1.83 mg/m<sup>2</sup>. Shear-yield stresses are proportional to B<sub>4</sub>C content. Solid lines show the behavior predicted by Herschel-Buckley model.

Finally, any dispersant used to form suspensions must be easy to remove during a binder burnout step. Thermogravimetric analysis results of PEI 25k (not shown) demonstrated that it can be completely removed with either argon or nitrogen atmospheres upon heating to 450°C. It should be noted that the oxidation of B<sub>4</sub>C starts at ~ 600°C, well above the 450°C burnout temperature.

A significant effort has been made to develop pressureless sintering processing approaches to make dense B<sub>4</sub>C parts. This work is ongoing, and the completed results will not be documented in this final report. However, subsequent publications will name ARO and this grant as supporting the research.

Groups of six dry-pressed B<sub>4</sub>C pellets with different sintering aids and amounts of sintering aid were pressureless sintered at 2000°C for 1 hour in an argon atmosphere. Of the six pellets sintered, one “reference” sample contained no sintering aids. The difference between the density of each of the five samples compared to the reference sample is shown in Figure 21. Note that the results in Figure 21 only include sintering aids that showed promising densification, e.g. 10 wt.% Y<sub>2</sub>O<sub>3</sub>, 8wt% ZrB<sub>2</sub> or SiC both, 3wt% Al<sub>2</sub>O<sub>3</sub>, 1wt% Al, and 0.5wt% Si .

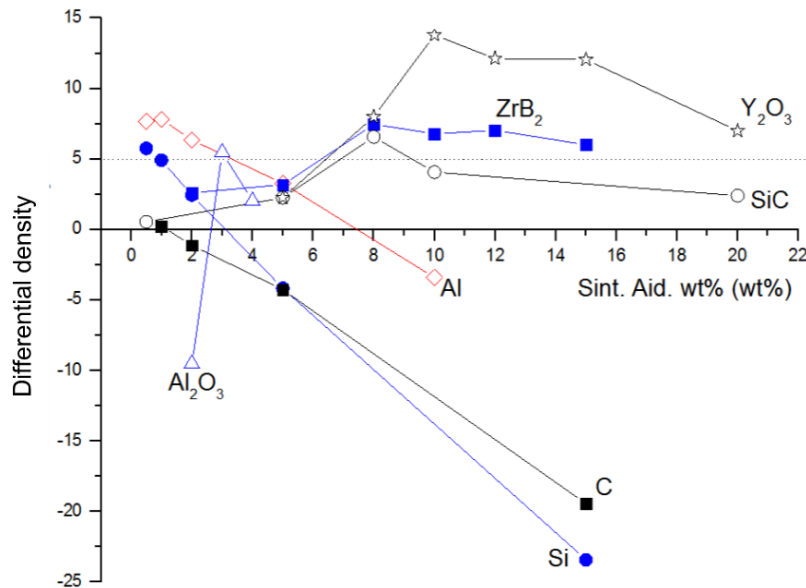


**Figure 21.** Percentage difference in density for each B<sub>4</sub>C pellet with sintering aid relative to a reference pellet (no sintering aids) after processing at 2000°C for 1 hr. The x-axis shows the concentration of the sintering aid. 10 wt.% Y<sub>2</sub>O<sub>3</sub> was among the best sintering aids studied.

The hardness of each B<sub>4</sub>C/sintering aid was measured using a Vicker’s indenter with a load of 1kg for 15 s. Although ZrB<sub>2</sub>, SiC, and Si samples shown higher relative densities than the reference sample, hardness values were below 20 GPa. Pellets with 10 wt.% Y<sub>2</sub>O<sub>3</sub>, 1 wt.% Al, and 3wt.% Al<sub>2</sub>O<sub>3</sub> had average hardnesses of 32.5, 27.7, and 26.2 GPa, respectively. Such samples were analyzed using SEM. Figure 22 shows the microstructures of samples using Al and Al<sub>2</sub>O<sub>3</sub> as sintering aids. Although samples have different sintering aids concentration, the Al atomic % for both sintering aids is close to 5 %.

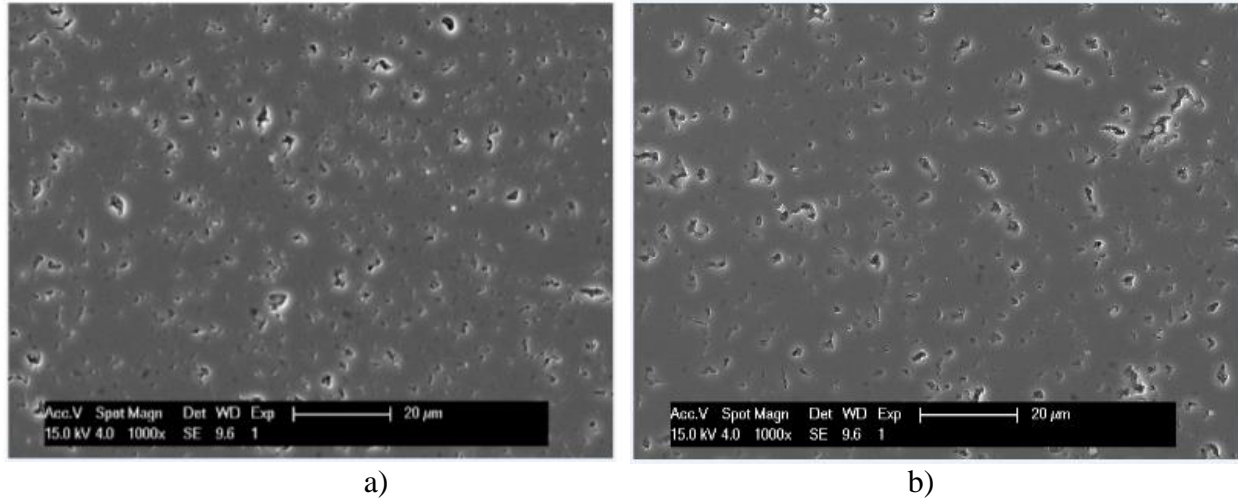


**Figure 22.** Microstructures of pellets using a) 1 wt% Al, and b) 3wt % Al<sub>2</sub>O<sub>3</sub> as sintering aids.

A representative region with 10 wt% Y<sub>2</sub>O<sub>3</sub> sintering aid is shown in Figure 23. Dark grey areas, labeled as “1” correspond to yttrium-rich phases. Light grey areas label as “2” correspond to WC contamination from attrition milling media. Yttrium, coming from reduced Y<sub>2</sub>O<sub>3</sub>, appears to melt (T<sub>m</sub> =1526°C) and fill the remaining porosity. The larger pores may be due to surface damage during polishing. In the next few months, Andres will prepare suspensions of B<sub>4</sub>C with Y<sub>2</sub>O<sub>3</sub> and begin injection molding.

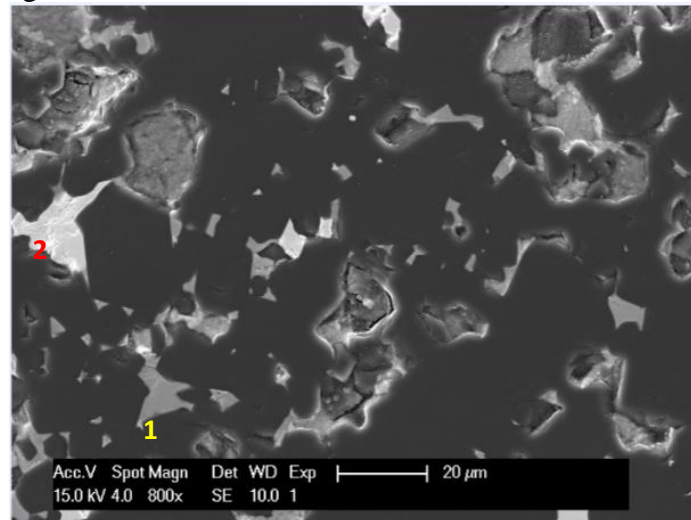


**Figure 23.** Microstructures of 10 wt% Y<sub>2</sub>O<sub>3</sub> sample. 1) Yttrium rich second phase. 2) WC from attrition milling media.